**Photosynthetic recovery in drought-rehydrated grapevines is associated with high demand from the sinks, maximizing the fruit-oriented performance**

The Plant Journal 2022

https://doi.org/10.1111/tpj.16000

Title:

**Photosynthetic recovery in drought-rehydrated grapevines is associated with high demand from the sinks, maximizing the fruit-oriented performance.**

Davide L. Patono[1], Daniel Said-Pullicino[1], Leandro Eloi Alcatrão[1], Andrea Firbus[1], Giorgio Ivaldi[1], Walter Chitarra[2,3], Alessandra Ferrandino[1], Davide Ricauda Aimonino[1], Luisella Celi[1], Giorgio Gambino[2], Irene Perrone[2], Claudio Lovisolo[1,2,*]

[1]Dept. Agricultural, Forest and Food Sciences, University of Turin, Grugliasco, Italy
[2]Institute for Sustainable Plant Protection, National Research Council, Turin, Italy
[3]Council for Agricultural Research and Economics-Research Centre for Viticulture and Enology (CREA-VE), Conegliano (TV), Italy
[*]Corresponding Author

SUMMARY

To understand how grapevine sinks compete with each other during water stress and subsequent rehydration, carbon (C) allocation patterns in drought-rehydrated vines (REC) at the beginning of fruit ripening were compared with control vines maintained under drought (WS) or fully irrigated (WW). In the 30 days following rehydration, the quantity and distribution of newly fixed C between leaves, roots and fruits was evaluated through $^{13}CO_2$ pulse-labelling and stable isotope ratio mass spectrometry.

REC plants diverted the same percentage of fixed C towards the berries as the WS plants, though higher than that of WW plants. Net photosynthesis (measured simultaneously with root respiration in a multi-chamber system for analysis of gas exchange above- and below-ground) was about twice in REC compared to WS treatment, and comparable or even higher than in WW plants. Maximizing C assimilation and delivery in REC plants led to a significantly higher amount of newly fixed C than in both control treatments, already two days after rehydration in root, and two days later in the berries, in line with the expression of genes responsible for sugar metabolism. In REC plants, the increase in C assimilation was able to support the requests of the sinks during fruit ripening, without affecting the reserves, as was the case in WS.

These mechanisms clarify what is experienced in fruit crops, when occasional rain or irrigation events are more effective in determining sugar delivery toward fruits, rather than constant and satisfactory water availabilities.

KEYWORDS

Water stress; drought; rehydration; $^{13}C$ pulse-chase technique; photosynthesis, respiration; sugar metabolism; sucrose synthase (*VvSusy*); cell wall invertase (*VvcwINV*); *Vitis vinifera* L.

SIGNIFICANCE STATEMENT

In the rehydration phases following a period of drought, the strength of fruit carbon sinks inherited from the previous period of stress persists in grapevines, coupled with a decisive photosynthetic recovery. These phases become the key moments in the life of fruit plants, especially if they coincide with the ripening phase of the fruit.

## INTRODUCTION

In temperate climate regions, rainfall is less evenly distributed during the growing season and the occurrence of prolonged periods of drought alternating with periods of abundant rainfall are increasing (Vilonen *et al*., 2022). In fleshy fruit crops, where the productivity and quality of fruits strictly depend on water availability, it is strategic to understand in more detail the dynamics of plant response to alternations between low and high water availability (Ripoll et al., 2014).

The adaptation of grapevines to water deficit and recovery is a complex biological process (Herrera et al., 2022), where the most explored response mechanisms are linked to the hydraulic adaptation of the vine (Perrone et al., 2012), to stomatal regulation (Lavoie-Lamoureux et al., 2017), and to their impact on photosynthesis (Galmés et al., 2007) and water use efficiency (Faralli et al., 2022). Decades of research

have focused on water transport in the event of drought stress (Lovisolo et al., 2010; Kuromori et al., 2022), while the transport of carbon (C) in the plant and the related metabolic activities of roots and shoots are less studied (Douthe et al., 2018; Gambetta et al., 2020).

Within plants, C source-sink relationships regulate photosynthate transport from sources towards other organs (sinks such as root tips, fruit and seeds) for further metabolism or storage. Currently there is a change in the paradigm from a source-limited model to a sink-limited model, source activity (photosynthesis) depending on sink activity (tissue growth) (Fatichi et al., 2014; Körner et al., 2015). In the last years, it has been demonstrated that photosynthetic activity in plants experiencing water stress is not only regulated by water transport, but is also controlled by the root C metabolism (Hasibeder et al., 2015). The first response of plants to the onset of water stress is the down-regulation of root respiration that leads to a lower unloading rate of sucrose from the phloem in root. This decrease in the flow rate results in an accumulation of sucrose in the leaf leading to a feedback inhibition of photosynthesis. Similarly, the recovery of root metabolic activity with rehydration is immediate, thus resolving the imbalance between production and use (Hagedorn et al., 2016; Rodrigues et al., 2019).

Plants have different sinks competing with each other for photo-assimilates, organized in a complex network (Knoblauch et al., 2016) that is based on a priority system, according to sink strengths (Ho, 2003), sink phenological phases, and environmental *stimuli* (Wardlaw, 1990). Photosynthetic performance and relative availability of C fluctuate throughout the day, as do phloem loading and source-sink regulation; although it is not yet clear how phloem cells perceive sugar concentration and modulate signalling and expression of transporters (e.g. Sugar Will Eventually be Exported Transporters – SWEET - genes) (Chen et al., 2012; Keller et al., 2021). In conditions of prolonged stress, such as drought, plants activate different adaptation responses that strongly influence the mobilization and transport of C and, in turn, the source-sink performance (Lemoine et al., 2013).

In contrast to tree species, fruit crops such as grapevines introduce more complexity in the C sink relations: the root sink activity intersects berry growth and ripening that attracts large amounts of C during the growing season, in particular during fruit ripening (in grapevine, after *veraison*), competing strongly with the roots (Pastenes et al., 2014). This derives from an ancestral need to convey nutrients to the seed with a parallel need to make the fruits palatable to the herbivore for seed dissemination that ensures the continuity of the progeny. Furthermore, the selection of the most productive phenotypes has made the fruit sink quantitatively competitive against the root sink (Ryan et al., 2018) to a greater extent than what is observed in forest plants, where roots completely orchestrate the response to stress (Hagedorn et al., 2016).

In this study, we aimed to explore whether the rehydration process could act as regulator of crop performance in an environment with low water availability and a highly-evapotranspirative atmosphere. It could be hypothesized that in crop fruit plants, which show an increasing fruit sink strength from flowering to harvest, the root carries out its sink activity secondary to the fruit. The object of our research is to understand when, how much and how the root and fruit compete with each other, and if during water stress and/or during the subsequent rehydration, the competition can be accentuated. To this end, we have conducted analyses through i) the assessment of C allocation kinetics in the different plant sinks (root-shoot-fruit) competing in drought and post-drought rehydrated vines, ii) the measurement of the ecophysiological performances in root and shoot, and iii) the analysis of transcripts of key genes involved in controlling source-sink interrelationships. Carbon allocation patterns between different sinks can be adequately studied by means of $^{13}C$ pulse-labelling approaches in which temporal changes in the $^{13}C$ isotope content of different plant parts after labelling with $^{13}C$ enriched $CO_2$ ($^{13}CO_2$) can be used to trace the distribution of neo-photosynthates and follow C partitioning between sinks (Epron et al., 2012).

## RESULTS

### Water treatments and gas exchange analysis

Since the beginning of March, three-year-old plants of grapevine *cv* Barbera with similar root volume were grown in pots and fully-irrigated (WW) to prevent water stress. At the end of July, 2/3 of the plants were exposed to water stress (WS) by drastically reducing the irrigation regime. On August 20$^{th}$ (day after re-hydration zero - DAR 0), one half of these plants were rehydrated (REC) to pre-stress conditions while the other half were maintained under water stress. A whole plant gas exchange analysis in a custom-built multi-chamber system was started one week before re-hydration. WW plants maintained a higher transpiration of the whole canopy (E, Figure 1a), net $CO_2$ assimilation of the whole canopy (A, Figure 1b), and belowground respiration ($R_{bg}$, Figure 2) than WS plants. While $R_{bg}$ of REC plants was rapidly restored to the level of WW plants within the first 2 h after rehydration, the levels of E and A of REC plants reached those of WW plants after 8 h. During the subsequent days, $R_{bg}$ and E of REC plants were comparable to those of WW plants. A of REC plants was similar to that of WW plants during DAR 1 and 2 with a trend of up-regulation in the central hours of the day that became statistically significant at DAR 3 and 4. From DAR 5 onwards, no differences in A between REC and WW plants were appreciable.

**Carbon allocation patterns to the different sinks following rehydration**

From 08.00 am to 12.00 am of DAR 1, nine plants (three for each treatment) were $^{13}CO_2$ pulse-labelled under climate-controlled conditions (Figure S1). Total $^{13}CO_2$ fixed by each plant immediately after labelling (DAR 1) corresponded to 9.2 ± 3.4 mmol $^{13}C$ plant$^{-1}$ that was found exclusively in the leaves, without significant differences among treatments. Up to 90% of this pool of newly assimilated C was rapidly lost from the leaves by respiration and reallocation to other plant parts within 2 d from labelling (DAR 3), irrespective of the irrigation regime. WW and WS leaves showed a slight further reduction of the residual $^{13}C$ at DAR 6 but no further significant loss of C was observable at DAR 15 and DAR 30. REC plants did not lose $^{13}C$ from leaves between DAR 3 and 6 but showed a decrease thereafter. By DAR 30 all plants showed the same residual amount of $^{13}C$ in the leaves that amounted to about 5-8% of assimilated C (Figure 3a).

Allocation of $^{13}C$ to the berries increased with time over the first days after labelling and subsequently reached a stable amount by DAR 6 to 15 (between 16 and 30% of fixed $^{13}C$) with no significant subsequent loss of $^{13}C$. However, whereas the maximum proportion of $^{13}C$ was reached within DAR 6 in WW and WS plants, $^{13}C$ allocation to the berries of REC plants continued to increase until DAR 15. The final proportion of $^{13}C$ allocated to the berries was higher in WS and REC plants with respect to WW ones (Figure 3b).

In contrast, $^{13}C$ allocation to the roots increased to a maximum by DAR 3 in WW, while in WS and REC root C allocation continued to increase slightly between DAR 3 and DAR 6. Subsequently, WW plants quickly lost $^{13}C$ between DAR 3 and 15 and all the $^{13}C$ remaining at DAR 15 persisted also at DAR 30. On the other hand, WS and REC plants showed a slower loss of $^{13}C$ that persisted also between DAR 15 and 30. By the end of the experiment, the residual proportion of fixed $^{13}C$ in the roots of WW, WS and REC plants (about 10 %) was not significantly different (Figure 3c).

Considering the total amount of fixed $^{13}C$ in the different pools, there was a strong decrease in fixed $^{13}C$ in the first 3 days that continued to decrease faster in WW plants with respect to WS and REC plants, resulting in a final proportion of fixed $^{13}C$ of about 40 % for WS and REC plants and 30 % for WW plants (Figure 3d).

Considering that the different irrigation treatments affected both net photosynthesis as well as the partitioning of newly assimilation C between the different sinks, we estimated the amount of C transferred to the sinks following re-hydration (DAR 0) by coupling daily integrals of A and total respiration ($R_{tot} = R_{bg} + R_{cd}$) at DAR 1 with the allocation of $^{13}C$ fixed at DAR 1 to the different sinks. In detail, plant gas exchange outputs at DAR 1 were integrated over 24 hours, and total daily A, $R_{bg}$, the respiration of the whole-canopy during dark hours ($R_{cd}$) and $R_{tot}$ are reported in table 1, showing that the ratio between $R_{tot}$ and A was significantly higher in WS plants than in WW and REC plants. We calculated the residual amount of C allocated to the different pools after sink respiration and/or re-mobilization by multiplying the proportion of residual $^{13}C$ in the different pools at DAR 1, 2, 3, 6, 15 and 30, with the integrated daily A of DAR 1 (the $^{13}C$ pulse day). Figure 4 reports this information and shows how total C allocated to berry and root was similar between WS and WW plants and higher in REC plants. Already from DAR 2 in root, and two days later in fruit, the amount of C in the REC treatment was significantly higher than in the control plants (both WW and WS). The WS plants allocated more C belowground than WW controls in the first 15 days, but then the consumption (respiration or translocation) brought the assimilated C to a level comparable to that of WW controls. Also in the REC roots, the maximum amount of C at DAR 6 tended to drop, indicating consumption and/or reallocation but the total amount of assimilated C that remained in the root at DAR 30 was significantly higher than WW and WS plants. On the contrary, C accumulation in the berries of REC plants remained stable and constant in time (Figure 4).

The amount of assimilated C that remained in the leaf at DAR 30 was much lower compared to the other two C pools, though nonetheless slightly higher in REC plants compared to WS and WW plants. Adding the total amounts of newly fixed C remaining in the roots, berries and leaves at DAR 30 to the daily $R_{tot}$ we observed that the amount of daily C assimilated was sufficient to support C accumulation and root and shoot respiration in WW and REC plants, but on the contrary, not sufficient in WS plants (Figure 5).

The accumulation levels of fresh and dry matter, measured at DAR 30 in berries, reflected the carbon fluxes described so far and the levels of water potential measured. The REC grapes generally showed higher levels than the WW ones, in turn higher than the WS ones (table 2).

**Transcript expression analyses of key genes involved in source-sink interrelationships**

The expression of different carbohydrate metabolism-related genes was analysed in source and sink tissues of WW, WS and REC plants over a time course characterizing the early phases after rewatering (DAR 0, DAR 1 and DAR4), in order to add information at the molecular level about carbon allocation dynamics (see Figures S2 a and b for DAR 0 and DAR 1 and Figure 6 for DAR 4. In general, the gene expression trends were similar during the early phases considered, thus we decided to describe more in detail the results occurring at DAR4 when ecophysiological measurements confirmed a fully recovery of REC plants (Figure 6). The sucrose synthase gene *VvSuSy* was expressed mainly in root and characterized by a lower expression level in WS treatment. An alternative route for sucrose breakdown in WS root was offered by the increased expression of the cell wall invertase (*VvcwINV*) gene, whose expression trend was in general

complementary to that of *VvSuSy* in WW, WS and REC root samples. Interestingly, WS root showed an increased expression of threalose-6-phosphate phosphatase (*VvTPP*) gene, responsible for the synthesis of threalose from the precursor threalose-6-phosphate. The availability of new photosynthates after rehydration allowed the REC root to increase the starch synthesis (*VvSTA*, starch synthase) mirroring the WW root behaviour, whereas in WS root *VvSTA* did not increase the expression level. This result agrees with the high hexose mobilization confirmed by the increased expression level of the hexose transporter 3 (*VvHT3*) in WS root in respect to the same tissue of WW and REC plants. In berry, two transcripts among the genes analysed showed high expression, mainly in WW and REC plants: the Sugar Will Eventually be Exported Transporter 10 (*VvSWEET10*), responsible for phloem unloading in sink tissues, and the vacuolar hexose transporter 6 (*VvHT6*) driving the carbohydrates to storage in the vacuole. Similarly, the vacuolar invertase *VvGIN2* showed expression in the berry reinforcing the sucrose compartmentalization in the vacuole (Figure 6).

## DISCUSSION

### Carbon balance in drought-rehydrated ripening grapevines

In this study, droughted vines rehydrated at *veraison* were pulse-labelled with $^{13}CO_2$ together with other vines maintained in water deficit or fully irrigated. The $^{13}C$ absorbed by the leaves with photosynthesis during labelling were subsequently used to trace the phloem flows of newly assimilated C towards the strongest sinks in the thirty days of the post-*veraison* phase, when the ripening processes of the grape occurred triggering C allocation towards the sinks. From the combined analysis of the $^{13}C$ allocation patterns, and photosynthesis and respiration gas exchanges of the plant (shoot and root) and rhizosphere compartments, we were able to demonstrate several interrelationships occurring among plant organs during a rehydration event following a drought period either above- or below-ground.

The resumption of root metabolic activity and post-rehydration photosynthesis is almost immediate (a few hours and less than 24 hours, respectively), showing how adapted the vine is to tolerate water stress. On the contrary, beech a mesophilic plant not adapted to arid climates (Fotelli et al., 2001), has been shown to take a few weeks for photosynthesis to recover to pre-stress conditions (Hagedorn et al. 2016), Furthermore, the presence in grapeveines of the fruit sink with considerable strength, triggered a photosynthetic and respiratory energy demand (Fatichi et al., 2014; Körner et al., 2015).

The water regime strongly influenced the partitioning of C towards the different sinks. Water stress caused a greater allocation of the newly photosynthesized carbonaceous resources to the berry (about double compared to WW controls), which are stored in a stable manner. On the other hand, the C allocated belowground over 30 days is mostly consumed. The plant in recovery diverts the same percentage of labelled C to the berry as the plants in water stress, although in absolute amounts its photosynthesis is about double that under water stress (it is comparable or even higher than photosynthesis in WW control plants). Therefore, the total C allocated to the berry is about 50% higher in recovery than in the irrigated control. These physiological mechanisms are at the basis of what is often experienced in irrigated fleshy fruit crops, where it has been previously shown that occasional irrigation events are more effective in determining sugar-related production, rather than maintaining a constant satisfactory water state (Chaves et al., 2010). Moreover, the rain fed areas with viticultural vocation present microclimatic situations of summer aridity with only occasional rains (Charrier et al., 2018).

Through a daily respired / photosynthesized C balance we show that during the ripening of the berry (30 days post *veraison*) 57% of the C assimilated in the irrigated condition is respired. In the same period, the accumulation of neo-photosynthates is about 28%, showing that plant photosynthesis can support C accumulation in sinks without affecting plant reserves accumulated pre-*veraison*, as showed Rossouw et al. (2017) in irrigated grapevines. On the contrary, upon water stress 83% of the daily C assimilated is respired; since 43% of neo-photosynthesized C is stored in a stable manner, we conclude that the plant should affect C radical reserves accumulated before *veraison* to support the respiration rate. After rehydration in REC pants, 54% of the daily C assimilated of the post-*veraison* month is respired, similarly to what happened in WW controls; about 43% of neo-photosynthesized C is stored in a stable manner (especially in berries), much more than under WW condition. However, the increase in A was able to support the requests of the sinks, without affecting the reserves, as was the case in WS. During WS, the lack of turgor acting as major limitation to growth (Hernandez-Santana et al., 2021) forced plants to affect C reserves, adding evidence to the sink limitation hypothesis to photosynthesis (Fatichi et al., 2014). The highest proportion of photosynthates was partitioned into fruits (berries) and it was in WS plants, almost double than under WW condition, as indicated by figure 5 (for fruits: daily C needs / daily C available: 27/176=15% in WW plants, 24/81=29% in WS plants and 45/188=23% in REC ones). From a wider point of view, this indicates why fruits are usually seen as stronger sinks than other organs or even how fruit growth is generally seen as less sensitive to water stress than vegetative growth.

**Molecular evidences supporting the model**

Delivery of labelled $^{13}C$ to the different sinks was observed in parallel with the expression of genes involved in carbohydrate metabolism. Genes encoding proteins that regulate the delivery of sucrose to the sinks and which catalyze the hydrolysis of the sucrose discharged to trigger respiration or carbon storage have been analysed. SuSy is an enzyme with a central role in the source-sink coordination, it catalyses the breakdown of sucrose in sink tissues to keep the concentration and pressure gradient operational in the phloem (Gessler, 2021). *SuSy* gene resulted expressed mainly in roots. In rehydrated roots, thanks to the availability of new photo-assimilated resources and the recovery of root respiration, the molecular machinery quickly adjusted to that of WW plants, whereas WS root showed a lower level of *SuSy* expression, probably to compensate the lack of assimilation. Interestingly, *cwINV* gene expression resulted significantly higher in WS root in respect to WW and REC roots, ensuring an alternative route of sucrose breakdown and the maintaining of the root sink strength also in water stress condition, as confirmed by the $^{13}C$ partitioning analysis. The relative impacts of SuSy and invertase on C allocation appears to be dependent on tissue, species, developmental stage and season (Dominguez *et al.*, 2021). Moreover, poplar RNAi transgenic lines for *SuSy* showed increased invertase activity, suggesting a partial compensation of the two enzymes in the sucrose cleavage activity, phenomenon that we can retrieve in our data also, looking at the complementary expression of *SuSy* and *cwINV* transcripts in the WW, WS and REC roots. The understanding of the reason why the grapevine root during water stress leans toward the preferential expression of the invertase requires further experiments. It is known that both pathways degrade sucrose but the products of their reactions differ considerably; the literature suggests that whereas SuSy could be involved in increased biomass (Gessler, 2021; Xu *et al.*, 2012), invertases could have a greater ability to stimulate specific sugar sensors (Ruan *et al.*, 2010; Ruan, 2012). The involvement of the water stressed root in the sucrose signalling was confirmed by the overexpression of the *threalose-6-phospate phosphatase* (TPP) transcript, catalysing the second step of threalose synthesis. Trehalose accumulation confers high tolerance levels to different abiotic stresses (Garg *et al.*, 2002) and, together with the precursor Threalose-6-phosphate, play key roles in the control of carbon allocation and of stress responses in plants (Morabito *et al.*, 2021). We could speculate that through the sugar signalling WS root orchestrated the maintaining of the sink strength despite the unfavorable conditions for C allocation. Hexoses produced from sucrose cleavage were not used for starch synthesis in WS root, as suggested by the low expression of *VvSTA* and the high expression of the *HT3*, confirming the mobilization of hexoses. On the contrary, the REC root started the starch synthesis quickly adjusting to the WW condition.

Sugar Will Eventually be Exported Transporters (SWEETs) 10 is a plasma membrane sucrose transporter of clade III SWEETs, deputated to the phloem unloading (Savoi *et al.*, 2021; Eom *et al.*, 2015). It is one of the two transcripts in our experiment expressed at high level in the berry. Although the main driver of sucrose unloading in the berry was the developmental stage (*veraison*), as suggested from the high *SWEET10* expression level over all the time course, a slight treatment effect could be noticed. Thanks to the photosynthesis and assimilation recovery, the REC plant was able to maximise the C allocation in the fruit. Interestingly, since *SWEET10* transcript level remained low in the REC root tissue, we can suggest that the prompt increase of root respiration after rehydration was not accompanied by an increase of the unloading rate of sucrose in root, differently from what happens in non-fruit trees (Hagedorn *et al.*, 2016). In grapevine, when the fruit is present, our experiment suggests that the root becomes a secondary sink. The unloading of sucrose was guaranteed by the *SWEET10* expression also in WS berries, although to a minor extent probably because of the limited photosynthates available in stress condition diverted also toward the root, as confirmed by *SWEET10* expression increasing in this tissue in respect to WW and REC plants. Finally, the analysis of the *vacuolar hexose transporter HT6* expression level, the second gene highly expressed in berry, pointed out that this transporter allowed the hexoses accumulation in the vacuole, so that the sink strength can be maintained to attract more C (as Susy does in root). Moreover, the storage of sucrose in the vacuole was driven also by the *vacuolar invertase GIN2*. In general, the berry metabolism appeared to be stopped as confirmed by the general low expression level of carbohydrate metabolism-related genes analyzed, with the exception of the genes described above that are key modulators for hexose and sucrose accumulation and cell expansion (Ruan *et al.*, 2010) in the phenological stage of *veraison*. This molecular difference underlines what has been seen in our C distribution model between the root and fruit sinks, which shows how the allocated C amount remains constant in the REC fruit over 30 days, and there is no redistributive decrease trend, as in the root.

**Possible implications of the research**

Confirming the measurements of carbon fluxes and water potential levels that plants experienced during the experiment, the berries of the REC plants were found to be the heaviest and with the highest sugar concentration at DAR 30. In WS plants, the low growth levels of the berries that developed in a context of scarce water availability were not coupled with low levels of sugar concentration (expressed in degree Brix), found significantly not lower than in the WW berries, confirming what shown as carbon accumulation in figure 4b.

Our experimental design mimicked a peculiar *scenario*, optimized to observe how much and how root and fruit compete with each other, but not necessarily aligned with what would be other possible *scenarios* in the field. It couples with a field situation, where mainly until *veraison* grapevines perceive water deficiency, followed by rain fed in the subsequent phases of the productive cycle. In this *scenario*, an increase of C allocation in berries positively regulates berry quality not only in relation to the accumulation of primary metabolites *per se*, but also to the accumulation of secondary metabolites as glycosides in the cell vacuoles (Ferrandino and Lovisolo, 2014). Furthermore, C and sugar biosynthesis-transport related genes couple with the activation of the phenylalanine ammonia lyase (PAL), the key enzyme of the phenylpropanoid pathway (Pirie and Mullins, 1976).

However, in some viticultural areas pre-*veraison* water deficits could be less frequent than water deficits later in the ripening process. Scholasch and Rienth (2019) reviewed water deficit-mediated changes in vine and berry physiology, highlighting how this latter *scenario*, opposite to what described by our experimental setup, could increase berry quality. This because reducing water availability after *veraison* positively affects yield components, via both a reduction of berry volume (Zúñiga et al., 2018) and the activation of ABA-related biosynthetic pathways (Ferrandino and Lovisolo, 2014). As a specular confirmation, Intrigliolo et al. (2016) showed that a post-*veraison* irrigation results in a 26-30% yield increase compared to rain fed vineyards that experienced a post-*veraison* water deficit.

In our work, the effects of the carbon distribution wave following rehydration coupled with the expected delivery of phloem-water. The genotype we used ('Barbera' on '420A') should mitigate the effects of a distinctly aniso-hydric response to water stress of the scion through the use of a rootstock that is not tolerant to drought, and therefore not inclined to force lowering of the water potential during drought (Tramontini et al., 2013; Lavoie-Lamoureux et al., 2017). In cases of varieties showing an aniso-hydric behavior grafted on tolerant rootstocks (for example descendants of *Vitis rupestris* L.), rehydration could have even more significant effects on the distribution wave of photosynthates; this is because the ability to compensate for the mechanisms of lowering the water potential (among all the osmotic adjustment and the control of embolism repair, Lovisolo et al., 2008b) in stressful situations would allow these phenotypes a fast and active post-rehydration recovery (Lovisolo et al., 2010; Scholasch and Rienth, 2019). By contrast, we can speculate that rehydration could be less effective in scions showing iso-hydric response to water deficit and/or rootstocks sensitive to drought (for example descendants of *Vitis riparia* L.) (Lovisolo et al., 2008b).

**Conclusions**

Our results show how periods of water stress activate a molecular response in the plant C sinks to compensate for the reduction in photosynthetic C assimilation. In fruit crops, the fruits compete strongly with the root. This derives from an ancestral need to convey nutrients to the seed with a parallel need to make the fruits palatable to the herbivore for a seed dissemination that ensures the continuity of the progeny. Furthermore, the selection of the most productive phenotypes has made the fruit sink quantitatively competitive against the root sink, much more than what happens in forest plants, where the root completely orchestrates the response to stress. In the rehydration phases, the strength of the sink persists but is coupled with a photosynthetic recovery activated by the phloem downloading capacity directed towards the strongest C-requesting sinks. This is so effective that the assimilation values of the rehydrated plants exceed those of the irrigated plants. In these moments, the effects of maximum C assimilation and relative delivery to the requesting sink take place. They therefore represent the key moments in the life of the fleshy fruit plants, especially if they coincide with the ripening phase of the fruit, as in our experimental design.

## EXPERIMENTAL PROCEDURES

**Plant material, growth condition and water stress treatment**

Plants of *Vitis vinifera cv* Barbera grafted onto *Vitis riparia* × *Vitis berlandieri* 420A rootstocks were grown for 3 years in 70 L pot. In February, vines were taken out from their growing pots, soil was removed and 24 plants with similar root volume were selected. Twelve selected vines were placed in 450 mm internal diameter and 450 mm deep custom metal pots with an air tight lid (for simultaneous measurement of $R_{bg}$ and whole plant gas exchange, Figure S3), while another 12 were transferred to 70 L plastic pots filled with 60 L of a 3:2 v/v sand-peat mixture and 9 g of grapevine granular fertilizer (12+12+17+2 MgO + 20 $SO_3$). Once the vines started to break dormancy, 4 shoots bearing a cluster were selected in each plant and, at the beginning of July, plant canopies were green-pruned to a similar leaf area (LA) (≈ 0,5 $m^2$).

During the growth season, 3 irrigation treatments were compared in order to have: 8 control plants (permanently well irrigated, WW), 8 water stress plant (exposed to water stress from the end of July to the end of the experiment, WS) and 8 rehydrated plants (exposed to water stress from the end of July to the 20$^{th}$ of August and after well irrigated till to the end of the experiment, REC). For each treatment we randomly selected 4 plants in plastic pots and 4 plants in metal pots. A moderate water deficit level (Lovisolo et al., 2010; Lavoie-Lamoureux et al., 2017; Rienth and Scholasch, 2019) was achieved in about one week at the

beginning of August and maintained until rehydration in REC plants and up to DAR 30 in WS plants. Water stress was achieved and maintained by progressively acting on soil moisture levels, checked gravimetrically approximately every two days. The design based on maintaining midday leaf water potential ($\Psi_{MD}$) levels, measured on detached leaves in the plants growing in metal pots by pressure chamber technique, weekly at the beginning of the imposition of water stress and more frequently as *veraison* approached. On REC plants, $\Psi_{MD}$ restored in one day after re-hydration, as expected (Lovisolo et al., 2008a) (Figure 7).

During the experiment after re-hydration the relative soil humidity (RSH) in WS pots ranged between 30 and 40% and also the pre-dawn leaf water potential ($\Psi_{PD}$) was checked (Rodriguez-Dominguez *et al*., 2022), and single leaf gas exchange at 10.00 am (Lovisolo *et al*., 2010) was assessed every two days to maintain the designed stress level by replenishing water losses accordingly. In WS plants $\Psi_{PD}$ was held around -0.18 ± 0.04 MPa, single leaf net $CO_2$ assimilation ($A_{leaf}$) around 4.7 ± 2.2 μmol of $CO_2$ $m^{-2}$ $s^{-1}$ and single leaf transpiration ($E_{leaf}$) around 1.2 ± 0.6 mmol of $H_2O$ $m^{-2}$ $s^{-1}$, while the well-watered (WW) condition corresponded to RSH>80%, $\Psi_{PD}$ of -0.05 ± 0.01 MPa, $A_{leaf}$ 10.3 ± 2.2 μmol of $CO_2$ $m^{-2}$ $s^{-1}$ and $E_{leaf}$ 3.0 ± 0.9 mmol of $H_2O$ $m^{-2}$ $s^{-1}$.

The rehydration was carried out on 20$^{th}$ August at 8.00 am restoring the pot RSH to 80%, similar to that constantly maintained in the control WW plants. In all measurements we performed, 20$^{th}$ August was considered the day after rehydration (DAR) zero (0) and has been designed in order to coincide with 100% berry *veraison*.

As a linear correlation was observed between the square leaf maximum width (diameter) and leaf area (LA) of Barbera grapevine (Figure S4), LA of each plant was estimated *in vivo* by measuring maximum diameter of all leaves according to Vitali *et al*. (2013). LA of plants for gas exchange analysis were calculated before and after the measurement campaign (at DAR -7 and at DAR 8) and LA of plants for carbon labelling were measured at DAR -1, 15 and 30.

At DAR 30, plants in plastic pots were entirely sampled, and leaf, berry and root fresh and dry biomass quantified. Weight of the berry, production of grapes per plant, number of berries per plant, degree Brix (°Brix) of the berries, and their total acidity as tartaric acid were assessed.

**Whole plant gas exchange measurements**

All the plants in the metal pots were installed in a multi-chamber system for continuous gas exchange analysis between whole-canopy, soil and atmosphere (Figure S3). Aboveground measurement consisted of 3 custom centrifuge fans (PBN, Italy) blowing atmospheric air into 12 polyethylene (Long Life, Eiffel, Italy) balloons through PVC pipelines. Centrifuge fan velocity was controlled with 3 inverters (VFD007EL23A, Delta, Taiwan) and air flow incoming into balloons was continuously monitored with hot-wire anemometers. Temperature inside the balloon was monitored with 12 thermocouples. For soil gas exchange measurements, air flow was supported by 3 diaphragm pumps (D7 series, Charles Austin, UK) pushing air into metal pots through pneumatic pipelines connected to the pot with pneumatic fittings. Air flow was continuously monitored with mass flow sensors (Top Trak 822, Sierra, USA). Air-volume homogenization was guaranteed by 12V fans in both balloons and metal pots. Pneumatic probes were positioned to balloons and metal pots outlets and to centrifuge fans inlet and connect to a $CO_2$ and $H_2O$ gas analyser (LI-850, LI-COR,USA). A manifold with 25 connections with a system of solenoid valves (320 series, Matrix, Italia) made possible to select the air sampling path.

In detail, there were 12 balloons divided into 3 modules; into each module from one to 2 plants per treatment were randomized. Measurements followed a repeated 120 s routine including 60 s of air purging and 60 s thereafter to determine the mean steady state value. The measurements were conducted following the sequence: 1 reference, 6 samples, 1 reference, 6 samples, 1 reference. Each routine consisted of 1 + 6 + 1 + 6 + 1 = 15 measurements * 120 s = 30 min. $H_2O$ and $CO_2$ were measured simultaneously. As for reference $CO_2$ (ranging between 405 and 425 ppm) there was greater stability than for reference $H_2O$ (ranging between 13 and 19 mbar), but by averaging the 3 references, a stable value was obtained. No gradient was observed when measuring the reference in the 3 modules.

Differential $CO_2$ concentration, differential $H_2O$ concentration and air flow were measured every 6 hours in the soil compartment.

All the electronic instrumentation was connected to a control system (Field Point, National Instruments, USA) and data collection was monitored with an external PC.

The single leaf respiration was measured in the night on replicate leaves with a portable infrared gas analyzer (GFS-3000, Walz, Germany) to estimate respiration of the whole-canopy during dark hours ($R_{cd}$). Whole-canopy A, E and $R_{cd}$, and belowground respiration ($R_{bg}$) were calculated following von Caemmerer and Farquhar's equations (von Caemmerer & Farquhar, 1981). Plant gas exchange measurements were performed in a period of high pressure and consequent highly-evapotranspirative atmosphere. Air temperature (T), photosynthetic photon flux density (PPFD) and air relative humidity (RH) were monitored and reported in Figure S5a, b, c.

**$^{13}CO_2$ pulse-labelling**

Three plants for each treatment were labelled with $^{13}CO_2$ at DAR 1 within an air-tight, transparent labelling chamber having an internal volume of 8.4 $m^3$. Before labelling the soil was sealed to minimize diffusion of the labelled $CO_2$ into the soil. During labelling the chamber temperature and relative humidity were set to 28°C and 60%, respectively, while natural light was integrated by artificial LED light. $CO_2$ concentration inside the chamber was monitored constantly with a portable IRGA that showed sensitivity to $^{13}CO_2$ that was previously determined to correspond to 11% of natural abundance $CO_2$. Labelling started at 8.00 am by repeatedly replacing $CO_2$ depleted by plant assimilation with 30 at% $^{13}CO_2$ generated through the reaction between 0.6 M $NaH^{13}CO_3$ (30 at%) and 4 M sulfuric acid to maintain the $CO_2$ concentrations in the chamber between 370-420 ppm throughout the labelling period (Figure S1). Plant labelling ended after 4 h after which tissue samples (leaves, berries and primary and secondary roots separated from a soil core) were immediately collected on all 9 labelled plants. In addition, three additional pots that remained unlabelled were sampled to provide the natural $\delta^{13}C$ background of plant compartments. All plant biomass samples were dried at 70°C, weighed, milled prior to $\delta^{13}C$ analysis. The same sampling procedure was performed at DAR 2, 3, 6, 15 and 30. After the pulse all 9+3 plants were enclosed in air ventilated balloon to reproduce the same condition of plant used for whole plant gas exchange analysis.

**Isotope ratio mass spectrometry (IRMS) measurements**

The $\delta^{13}C$ values and C contents of plant biomass samples were measured by high-temperature combustion in an elemental analyser (Vario Isotope Select, Elementar Analysensysteme GmbH, Hanau, Germany) coupled to an isotope ratio mass spectrometer (Isoprime 100, Elementar). The $\delta^{13}C$-values (‰) were calibrated relative to the international standard Vienna Pee Dee Belemnite (VPDB) by means of a three-point calibration using standard reference materials IAEA-600, IAEA-603 and IAEA-CH3. Measurement uncertainty was monitored by repeated measurements of internal laboratory standards and standard reference materials. Precision was determined to be ±0.1‰ based on repeated measurements of calibration standards and internal laboratory standards. Accuracy was determined to be ±0.1‰ on the basis of the difference between the observed and known δ values of check standards and their standard deviations. The total analytical uncertainty for $\delta^{13}C$ values was estimated to be ±0.2‰. To estimate $^{13}CO_2$ uptake by leaves and translocation to other organs, δ notations were first expressed in atom%, and subsequently the C content of an organ fraction was multiplied by with the $^{13}C$ excess (atom%) of this fraction (with respect to the $^{13}C$ of the unlabelled control), as follows:

$$^{13}\text{C fixed (mg plant}^{-1}) = \frac{(\text{at\%}\,^{13}C_{\text{labelled}} - \text{at\%}\,^{13}C_{\text{unlabelled}})}{100} \cdot B \cdot \frac{C\%}{100}$$

Where B is the dry weight (DW) of plant biomass compartments (leaf, root or berry) and C% is the percentage of C in the sample. Changes in the total amounts of $^{13}C$ assimilated or delivered in the different plant organs with time were expressed as a percentage of the amount of $^{13}C$ fixed by the leaves at DAR 1 (the labelled $^{13}C$), assumed to represent the total $^{13}C$ assimilated by the plant during labelling.

To model the total amount of C assimilated at DAR 1 that was directed to the different C pools and that persisted during the experimental period, we multiplied the integral amount of C assimilated at DAR 1 to the percentage of C partitioning determined from the $^{13}CO_2$ pulse labelling.

$$C\ \text{allocation}_{\text{pool, t}}\ [\text{mmol C}] = \text{Daily } A_{\text{DAR 1}}\ [\text{mmol}] * {}^{13}C_{\text{pool, t}}\ [\%]$$

Where C $\text{allocation}_{\text{pool, t}}$ is the total C assimilated at DAR 1 that is allocated and persisted at time t in the considered pool. Daily $A_{\text{DAR 1}}$ is the integral of daily C assimilated at DAR 1. $^{13}C_{\text{pool, t}}$ is the percentage of the amount of $^{13}C$ fixed by the leaves at DAR 1, that is present in the C pool at time t.

Leaf biomass was calculated using the linear correlation that exist between leaf diameter$^2$ and leaf DW (Figure S4), plant leaf diameters were measured at DAR 0, 6, 15 and 30. Root biomass was dried and weighted at DAR 30, no evidence of root growth were observed for WS plants, but only for WW and REC plants (root lighter in colour with white root tips). In any case, the volume of new roots on the total root volume was negligible. For each plant a representative portion of the total root system was exanimated, primary and secondary roots were manually separated and weighted and the relative weight was normalized to the total weight of the root system. Total fruit dry mass was quantified at DAR 30. Average DW of berries sampled at DAR 1, 2 and 3 for each plant were compared to average DW of berries sampled at DAR 30. An 18 % increase of berry DW was observed and it was linearly distributed along the 30 days monitored. No difference in berry DW were observed between treatments.

**Molecular analysis**

At 4 hours (DAR 0), at 28 hours (DAR 1), and at 4 days from rewatering (DAR 4), at 12.00 am, leaf, berry and root samples collected from WW, WS and REC plants (3 biological replicates for each treatment) were sampled in liquid nitrogen. Plant materials were ground in liquid nitrogen; 40 mg of leaf and 200 mg of root

and berry were used for total RNA extraction with Spectrum Plant Total RNA kit (Sigma Aldrich, USA). cDNA was synthesized from 1 μg of the total RNA with High Capacity cDNA Reverse Transcription Kit (Life Technologies, USA). RT-qPCR analyses were performed as described before (Chitarra et al., 2017), using the oligonucleotide sets listed in Table S1. Three technical replicates were run for each biological replicate, and the expression of transcripts was quantified after normalization to two housekeeping genes: ubiquitin (VvUBI) and actin (VvACT). One-way analyses of variance (ANOVA) with treatment as the main factor were performed with the SPSS 23.0 statistical software package (SPSS Inc., Cary, NC, USA). Tukey's HSD-test was applied when ANOVA showed significant differences ($P < 0.05$). The standard error of all means was calculated.

ACKNOWLEDGEMENTS

The authors thank Klaas De Backer, Samuele Bolassa, Corrado Domanda, Cristina Lerda, Emilio Dicembrini, Mauro Caviglione, Marco D'Oria for technical help during experiments. Financial support: CARBOSTRESS project – CRT - Cassa Risparmio Torino Foundation.

AUTHOR CONTRIBUTIONS

DLP, DSP, IP and CL conceptualized and wrote the original draft. DLP, DSP, LEA, GI, AFi, IP carried out the experimental part under supervision from GG, DRA, AFe, LC, CL. GG, WC, AFe critically reviewed the draft. All authors read and approved the manuscript.

CONFLICT OF INTERESTS

The authors declare that they have no competing interests.

DATA AVAILABILITY STATEMENT

All relevant data can be found within the manuscript and its supporting materials.

SUPPORTING INFORMATION

Additional Supporting Information may be found in the online version of this article.

Table S1. List of the oligonucleotides used in this study.
Figure S1. $^{13}CO_2$ pulse of nine grapevine plants under climate-controlled condition at DAR 1 in the labelling chamber.
Figures S2. Transcripts of key genes of sugar metabolism. Relative expression level of (a) sucrose synthase (*VvSusy*), cell wall invertase (*VvcwINV*), threalose-6-phosphate phosphatase (*VvTPP*), starch synthase (*VvSTA*), and (b) hexose transporter 3 (*VvHT3*), Sugar Will Eventually be Exported Transporter 10 (*VvSWEET10*), hexose transporter 6 (*VvHT6*) and vacuolar invertase 2 (*VvGIN2*) genes in leaf, root and berry tissues sampled from WW, WS and REC plants at DAR 0 and DAR1.
Figure S3. Multichamber system for continuous gas exchange analysis.
Figure S4. Leaf area (LA) index of *Vitis vinifera cv* Barbera grafted onto *Vitis riparia* × *Vitis berlandieri* 420A rootstocks.
Figure S5. Environmental check during the whole-plant gas exchange analysis. (a) air temperature, T; (b) photosynthetic photon flux density, PPFD; (c) air relative humidity, RH.

REFERENCES

**Caemmerer, S. von and Farquhar, G.D.** (1981) Some relationships between the biochemistry of photosynthesis and the gas exchange of leaves. *Planta*, **153**, 376–387.

**Charrier, G., Delzon, S., Domec, J.-C., Zhang, L., Delmas, C.E.L., Merlin, I., Corso, D., King, A., Ojeda, H., Ollat, N., Prieto, J. A., Scholach, T., Skinner, P., van Leeuwen, C. and Gambetta, G. A.** (2018) Drought will not leave your glass empty: Low risk of hydraulic failure revealed by long-term drought observations in world's top wine regions. *Science Advances*, **4**, eaao6969.

**Chaves, M.M., Zarrouk, O., Francisco, R., Costa, J.M., Santos, T., Regalado, A.P., Rodrigues, M.L. and Lopes, C.M.** (2010) Grapevine under deficit irrigation: hints from physiological and molecular data. *Annals of Botany*, **105**, 661–676.

**Chen, L.-Q., Qu, X.-Q., Hou, B.-H., Sosso, D., Osorio, S., Fernie, A.R. and Frommer, W.B.** (2012) Sucrose efflux mediated by SWEET proteins as a key step for phloem transport. *Science*, **335**, 207–211.

**Chitarra, W., Perrone, I., Avanzato, C.G., Chitarra, W., Perrone, I., Avanzato, C. G., Minio, A., Boccacci, P., Santini, D., Gilardi, G., Siciliano, I., Gullino, M.L., Delledonne, M., Mannini, F. and Gambino, G.** (2017) Grapevine Grafting: Scion Transcript Profiling and Defense-Related Metabolites Induced by Rootstocks. *Frontiers in Plant Science*, **8**. Available at: https://www.frontiersin.org/article/10.3389/fpls.2017.00654 [Accessed June 13, 2022].

**Dominguez, P.G., Donev, E., Derba-Maceluch, M., Bünder, A., Hedenström, M., Tomášková, I., Mellerowicz, E.J. and Niittylä, T.** (2021) Sucrose synthase determines carbon allocation in developing wood and alters carbon flow at the whole tree level in aspen. *New Phytologist*, **229**, 186–198.

**Douthe, C., Medrano, H., Tortosa, I., Escalona, J.M., Hernández-Montes, E. and Pou, A.** (2018) Whole-Plant Water Use in Field Grown Grapevine: Seasonal and Environmental Effects on Water and Carbon Balance. *Frontiers in Plant Science*, **9**. Available at: https://www.frontiersin.org/article/10.3389/fpls.2018.01540 [Accessed June 13, 2022].

**Eom, J.-S., Chen, L.-Q., Sosso, D., Julius, B.T., Lin, I.W., Qu, X.-Q., Braun, D.M. and Frommer, W.B.** (2015) SWEETs, transporters for intracellular and intercellular sugar translocation. *Current Opinion in Plant Biology*, **25**, 53–62.

**Epron, D., Bahn, M., Derrien, D., Lattanzi, F. A., Pumpanen, J., Gessler, A., Högberg, P., Maillard, P., Dannoura, M., Gérant, D. and Buchmann, N.** (2012) Pulse-labelling trees to study carbon allocation dynamics: a review of methods, current knowledge and future prospects. *Tree Physiology*, **32**, 776–798.

**Faralli, M., Bontempo, L., Bianchedi, P. L., Moser, C., Bertamini, M., Lawson, T., Camin, F., Stefanini, M. and Varotto, C.** (2022) Natural variation in stomatal dynamics drives divergence in heat stress tolerance and contributes to the seasonal intrinsic water-use efficiency in *Vitis vinifera* (subsp. *sativa* and *sylvestris*). *Journal of Experimental Botany*, **73**, 3238-3250.

**Fatichi, S., Leuzinger, S. and Körner, C.** (2014) Moving beyond photosynthesis: from carbon source to sink-driven vegetation modeling. *New Phytologist*, **201**, 1086–1095.

**Ferrandino, A. and Lovisolo, C.** (2014) Abiotic stress effects on grapevine (*Vitis vinifera* L.): focus on abscisic acid-mediated consequences on secondary metabolism and berry quality. *Environmental and Experimental Botany* **103**, 138–147. Available at: https://doi.org/10.1016/j.envexpbot.2013.10.012

**Fotelli, M.N., Geßler, A., Peuke, A.D. and Rennenberg, H.** (2001) Drought affects the competitive interactions between Fagus sylvatica seedlings and an early successional species, Rubus fruticosus: responses of growth, water status and δ13C composition. *New Phytologist*, **151**, 427–435.

**Galmés, J., Medrano, H. and Flexas, J.** (2007) Photosynthetic limitations in response to water stress and recovery in Mediterranean plants with different growth forms. *New Phytologist*, **175**, 81–93.

**Gambetta, G.A., Herrera, J.C., Dayer, S., Feng, Q., Hochberg, U. and Castellarin, S.D.** (2020) The physiology of drought stress in grapevine: towards an integrative definition of drought tolerance. *Journal of Experimental Botany,* **71**, 4658–4676.

**Garg, A.K., Kim, J.-K., Owens, T.G., Ranwala, A.P., Choi, Y.D., Kochian, L.V. and Wu, R.J.** (2002) Trehalose accumulation in rice plants confers high tolerance levels to different abiotic stresses. *Proceedings of the National Academy of Sciences*, **99**, 15898–15903.

**Gessler, A.** (2021) Sucrose synthase – an enzyme with a central role in the source–sink coordination and carbon flow in trees. *New Phytologist*, **229**, 8–10.

**Hagedorn, F., Joseph, J., Peter, M., Luster, J., Pritsch, K., Geppert, U., Kerner, R., Molinier, V., Egli, S., Schaub, M., Liu, J. -F., Li, M., Sever, K., Weiler, M., Siegwolf, R. T. W., Gessler, A. and Arend M.** (2016) Recovery of trees from drought depends on belowground sink control. *Nature Plants*, **2**, 16111.

**Hasibeder, R., Fuchslueger, L., Richter, A. and Bahn, M.** (2015) Summer drought alters carbon allocation to roots and root respiration in mountain grassland. *New Phytologist*, **205**, 1117–1127.

**Hernandez-Santana, V., Perez-Arcoiza, A., Gomez-Jimenez, M.C. and Diaz-Espejo, A.** (2021) Disentangling the link between leaf photosynthesis and turgor in fruit growth. *The Plant Journal*, **107**, 1788-1801. Available at: https://doi.org/10.1111/tpj.15418

**Herrera, J.C., Calderan, A., Gambetta, G.A., Peterlunger, E., Forneck, A., Sivilotti, P., Cochard, H. and Hochberg, U.** (2022) Stomatal responses in grapevine become increasingly more tolerant to low water potentials throughout the growing season. *The Plant Journal*, **109**, 804–815.

**Ho, L.C.** (2003) Metabolism And Compartmentation Of Imported Sugars In Sink Organs In Relation To Sink Strength. *Annual Review of Plant Physiology and Plant Molecular Biology*, **39**, 355–378.

**Intrigliolo, D.S., Lizama. V., García-Esparza, M.J., Abrisqueta I. and Álvarez I.** (2016) Effects of postveraison irrigation regime on Cabernet-Sauvignon grapevines in Valencia, Spain: Yield and grape composition. *Agricultural Water Management*, **170**, 110-119. Available at: https://doi:10.1016/j.agwat.2015.10.020

**Keller, I., Rodrigues, C.M., Neuhaus, H.E. and Pommerrenig, B.** (2021) Improved resource allocation and stabilization of yield under abiotic stress. *Journal of Plant Physiology*, **257**, 153336.

**Körner, C.** (2015) Paradigm shift in plant growth control. *Current Opinion in Plant Biology,* **25**, 107–114.

**Knoblauch, M., Knoblauch, J., Mullendore, D.L., Savage, J.A., Babst, B.A., Beecher, S.D., Dodgen, A.C., Jensen, K.H. and Holbrook, N.M.** (2016) Testing the Münch hypothesis of long distance phloem transport in plants C. S. Hardtke, ed. *eLife*, **5**, e15341.

**Kuromori, T., Fujita, M., Takahashi, F., Yamaguchi-Shinozaki, K., and Shinozaki, K.** (2022) Inter-tissue and inter-organ signaling in drought stress response and phenotyping of drought tolerance. *The Plant Journal*, **109**, 342–358. Available at: https://doi.org/10.1111/tpj.15619

**Lavoie-Lamoureux, A., Sacco, D., Risse, P.-A. and Lovisolo, C.** (2017) Factors influencing stomatal conductance in response to water availability in grapevine: a meta-analysis. *Physiologia Plantarum*, **159**, 468–482.

**Lemoine, R., La Camera, S., Atanassova, R., Dédaldéchamp, F., Allario, T., Pourtau, N., Bonnemain, J. -L., Laloi, M. Coutos-Thévenot, P., Maurousset, L, Faucher, M., Girousse, C., Lemonnier, P., Parrilla, J. and Durand, M.** (2013) Source-to-sink transport of sugar and regulation by environmental factors. *Frontiers in Plant Science*, **4**. Available at: https://www.frontiersin.org/article/10.3389/fpls.2013.00272 [Accessed June 13, 2022].

**Lovisolo, C., Perrone, I., Carra, A., Ferrandino, A., Flexas, J., Medrano, H. and Schubert, A.** (2010) Drought-induced changes in development and function of grapevine (Vitis spp.) organs and in their hydraulic and non-hydraulic interactions at the whole-plant level: a physiological and molecular update. *Functional Plant Biology*, **37**, 98–116.

**Lovisolo, C., Perrone, I., Hartung, W. and Schubert, A.** (2008a) An abscisic acid-related reduced transpiration promotes gradual embolism repair when grapevines are rehydrated after drought. *New Phytologist*, **180**, 642–651. Available at: https://doi.org/10.1111/j.1469-8137.2008.02592.x

**Lovisolo, C., Tramontini, S, Flexas, J. and Schubert, A.** (2008b) Mercurial inhibition of root hydraulic conductance in *Vitis* spp. rootstocks under water stress. *Environmental and Experimental Botany*, **63**,178-182. Available at: https://doi.org/10.1016/j.envexpbot.2007.11.005

**Morabito, C., Secchi, F. and Schubert, A.** (2021) Grapevine TPS (trehalose-6-phosphate synthase) family genes are differentially regulated during development, upon sugar treatment and drought stress. *Plant Physiology and Biochemistry*, **164**, 54–62.

**Pastenes, C., Villalobos, L., Ríos, N., Reyes, F., Turgeon, R. and Franck, N.** (2014) Carbon partitioning to berries in water stressed grapevines: The role of active transport in leaves and fruits. *Environmental and Experimental Botany*, **107**, 154–166.

**Perrone, I., Pagliarani, C., Lovisolo, C., Chitarra, W., Roman, F. and Schubert, A.** (2012) Recovery from water stress affects grape leaf petiole transcriptome. *Planta*, **235**, 1383–1396.

**Pirie, A. and Mullins, M.G.** (1976) Changes in anthocyanin and phenolics content of grapevine leaf and fruit tissues treated with sucrose, nitrate, and abscisic acid. *Plant Physiology* **58**, 468-472.

**Rienth, M. and Scholasch, T.** (2019) State-of-the-art of tools and methods to assess vine water status. *OENO One*, **53**, 619-637. Available at: https://doi.org/10.20870/oeno-one.2019.53.4.2403

**Ripoll, J., Urban, L., Staudt, M., Lopez-Lauri, F., Bidel, L.P.R. and Bertin, N.** (2014) Water shortage and quality of fleshy fruits--making the most of the unavoidable. *Journal of Experimental Botany*, **65**, 4097–4117.

**Rodrigues, J., Inzé, D., Nelissen, H. and Saibo, N.J.M.** (2019) Source–Sink Regulation in Crops under Water Deficit. *Trends in Plant Science*, **0**. Available at: https://www.cell.com/trends/plant-science/abstract/S1360-1385(19)30101-3 [Accessed June 15, 2019].

**Rodriguez-Dominguez, C.M., Forner, A., Martorell, S., Choat, B., Lopez, R., Peters, J. M. R., Pfautsch, S., Mayr, S., Carins-Murphy, M.R., McAdam, S. A. M., Richardson, F., Diaz-Espejo, A., Hernandez-Santana, V., Menezes-Silva, P. E., Torres-Ruiz, J. M., Batz T. A. and Sack L.** (2022) Leaf water potential measurements using the pressure chamber: Synthetic testing of assumptions towards best practices for precision and accuracy. *Plant, Cell & Environment*, **45, 2037–2061.**

**Rossouw, G.C., Smith, J.P., Barril, C., Deloire, A. and Holzapfel, B.P.** (2017) Carbohydrate distribution during berry ripening of potted grapevines: Impact of water availability and leaf-to-fruit ratio. *Scientia Horticulturae*, **216**, 215–225.

**Ruan, Y.-L.** (2012) Signaling role of sucrose metabolism in development. *Molecular Plant*, **5**, 763–765.

**Ruan, Y.-L., Jin, Y., Yang, Y.-J., Li, G.-J. and Boyer, J.S.** (2010) Sugar input, metabolism, and signaling mediated by invertase: roles in development, yield potential, and response to drought and heat. *Molecular Plant*, **3**, 942–955.

**Ryan, M.G., Oren, R. and Waring, R.H.** (2018) Fruiting and sink competition. *Tree Physiology*, **38**, 1261–1266.

**Savoi, S., Torregrosa, L. and Romieu, C.** (2021) Transcripts switched off at the stop of phloem unloading highlight the energy efficiency of sugar import in the ripening V. vinifera fruit. *Horticulture Research*, **8**, 1–15.

**Scholasch, T. and Rienth, M.** (2019) Review of water deficit mediated changes in vine and berry physiology; Consequences for the optimization of irrigation strategies. *OENO One*, **53**, 423-444. Available at: https://doi.org/10.20870/oeno-one.2019.53.3.2407

**Tramontini, S., Vitali, M., Centioni, L., Schubert, A. and Lovisolo, C.** (2013) Rootstock control of scion response to water stress in grapevine. *Environmental and Experimental Botany* **93**, 20–26. Available at: https://doi.org/10.1016/j.envexpbot.2013.04.001

**Vilonen, L., Ross, M. and Smith, M.D.** (2022) What happens after drought ends: synthesizing terms and definitions. *New Phytologist*, Available at: https://onlinelibrary.wiley.com/doi/abs/10.1111/nph.18137 [Accessed June 13, 2022].

**Vitali, M., Tamagnone, M., Iacona, T.L. and Lovisolo, C.** (2013) Measurement of grapevine canopy leaf area by using an ultrasonic-based method. *OENO One*, **47**, 183–189.

**Wardlaw, I.F.** (1990) Tansley Review No. 27 The control of carbon partitioning in plants. *New Phytologist*, **116**, 341–381.

**Xu, C., Yin, X., Lv, Y., Wu, C., Zhang, Y. and Song, T.** (2012) A near-null magnetic field affects cryptochrome-related hypocotyl growth and flowering in Arabidopsis. *Advances in Space Results*, **49**, 834–840.

**Zúñiga, M., Ortega-Farías, S., Fuentes, S., Riveros-Burgos, C. and Poblete-Echeverría. C.** (2018) Effects of Three Irrigation Strategies on Gas Exchange Relationships, Plant Water Status, Yield Components and Water Productivity on Grafted Carménère Grapevines. *Frontiers in Plant Science*, **9**, 992. Available at: https://doi.org/10.3389/fpls.2018.00992

Table 1. Gas exchange integrals at DAR 1. Daily integrals of: whole-canopy assimilation (A), respiration of the whole-canopy during dark hours ($R_{cd}$), belowground respiration ($R_{bg}$), total respiration ($R_{tot} = R_{bg} + R_{cd}$) at DAR 1. Values are means ± SE (*n*=4). Statistical analysis of data was performed using the one-way analysis of variance (ANOVA) followed by a *post hoc* Tukey's test. Letters denote statistically significant variations ($p < 0.05$).

| | Daily A | Daily $R_{bg}$ | Daily $R_{cd}$ | Daily $R_{tot}$ | $R_{tot}$/A |
|---|---|---|---|---|---|
| | mmol $CO_2$ | mmol $CO_2$ | mmol $CO_2$ | mmol $CO_2$ | % |
| WW | 176 ± 14 a | 92 ± 10 a | 9 ± 1 a | 101 ± 9 a | 57 ± 2 b |
| WS | 81 ± 10 b | 59 ± 5 b | 8 ± 1 a | 67 ± 6 b | 83 ± 4 a |
| REC | 188 ± 33 a | 90 ± 2 a | 9 ± 1 a | 100 ± 2 a | 54 ± 8 b |

Table 2. Weight of the berry (g), production of grapes per plant (kg), number of berries per plant (#), degree Brix (°Brix), total acidity as tartaric acid (g $L^{-}1$) measured on DAR 30. Values are means ± SE (*n*=4). Statistical analysis of data was performed using the one-way analysis of variance (ANOVA) followed by a *post hoc* Tukey's test. Letters denote statistically significant variations ($p < 0.05$).

| | Weight of the berry | Production of grapes per plant | Number of berries per plant | °Brix | Total acidity as tartaric acid |
|---|---|---|---|---|---|
| | g | kg | | | g L-1 |
| WW | 1.80 ± 0.14 b | 0.34 ± 0.02 b | 192 ± 15 a | 24.5 ± 0.46 b | 8.00 ± 0.35 a |
| WS | 1.53 ± 0.09 c | 0.29 ± 0.05 c | 192 ± 33 a | 23.8 ± 0.63 b | 6.65 ± 0.66 a |
| REC | 2.27 ± 0.04 a | 0.47 ± 0.04 a | 205 ± 36 a | 25.6 ± 0.36 a | 7.25 ± 0.43 a |

**FIGURE LEGENDS**

Figure 1. Whole-plant gas exchange analysis. (a) transpiration, E and (b) net photosynthesis, A. From DAR -5 to DAR -1 data of WW (black squares, *n*=4) and WS (white circles, *n*=8) plants before the rehydration event are represented; from DAR 0 to DAR 7 data of WW (*n*=4), WS (*n*=4) and REC (grey triangles, *n*=4) plants after rehydration are plotted. Dotted vertical lines before and after DAR 0 show re-hydration and $^{13}CO_2$ pulse-labelling. Statistical analysis of data was performed using the one-way analysis of variance (ANOVA) followed by a *post hoc* Tukey's test. Letters in the table denote statistically significant variations ($p < 0.05$).

Figure 2. Whole-plant gas exchange analysis. Belowground respiration ($R_{bg}$). Symbols, replicates (*n*) and statistical analysis as in Figure 1.

Figure 3. $^{13}C$ partitioning of neo-photosynthates after a re-hydration event. Partitioning of assimilated labelled $^{13}CO_2$ during feeding event at DAR 1. (a), (b), (c), (d) represent % of labelled $^{13}C$ at DAR 1, 2, 3, 6, 15, 30 respectively in leaf, berry, root and whole plant. Values are means ± SE (*n*=3). Statistical analysis of data was performed using the one-way analysis of variance (ANOVA) followed by a *post hoc* Tukey's test. Letters in the table denote statistically significant variations ($p < 0.05$).

Figure 4. Carbon accumulation. Amounts of carbon allocations in different sinks obtained by multiplying the residual $^{13}C$ percent found in the different pools at DAR 1, 2, 3, 6, 15 and 30 with the integrated daily A of DAR 1 (the $^{13}C$ pulse day) in the leaf canopy (a), in all berries (b), and in the whole root (c). Values are means ± SE (*n*=3). Statistical analysis of data was performed using the one-way analysis of variance (ANOVA) followed by a *post hoc* Tukey's test. Letters in the table denote statistically significant variations ($p < 0.05$).

Figure 5. Model of C allocation to different C pools. The model is the combination of data from gas exchange analysis with data from pulse-chasing C isotope analysis. In blue, yellow and grey we showed the amount of neo-photosynthates that will be permanently stocked respectively in root, berries and leaf C pools. In orange and green, daily $R_{tot}$ and daily A is reported.

Figure 6. Transcripts of key genes of sugar metabolism. Relative expression level of sucrose synthase (*VvSusy*), cell wall invertase (*VvcwINV*), threalose-6-phosphate phosphatase (*VvTPP*), starch synthase (*VvSTA*), hexose transporter 3 (*VvHT3*), Sugar Will Eventually be Exported Transporter 10 (*VvSWEET10*), hexose transporter 6 (*VvHT6*) and vacuolar invertase 2 (*VvGIN2*) genes in leaf, root and berry tissues sampled from WW, WS and REC plants at DAR 4, as determined by qRT-PCR signals normalized to actin (*VvACT*) and ubiquitin (*VvUBI*) transcripts. Data are presented as the mean ±SE of three biological and technical replicates. Gene IDs and oligonucleotides used for each gene are indicated in the Table S1. Different lowercase letters above the bars indicate significant differences according to a *post hoc* Tukey's test ($p \leq 0.05$).

Figure 7. Imposition and maintenance of water deficit levels. Relative soil humidity measured gravimetrically, and midday leaf water potential measured by pressure chamber technique on detached leaves. Values are means ± SE (*n*=4).

1 Figure 1.
2

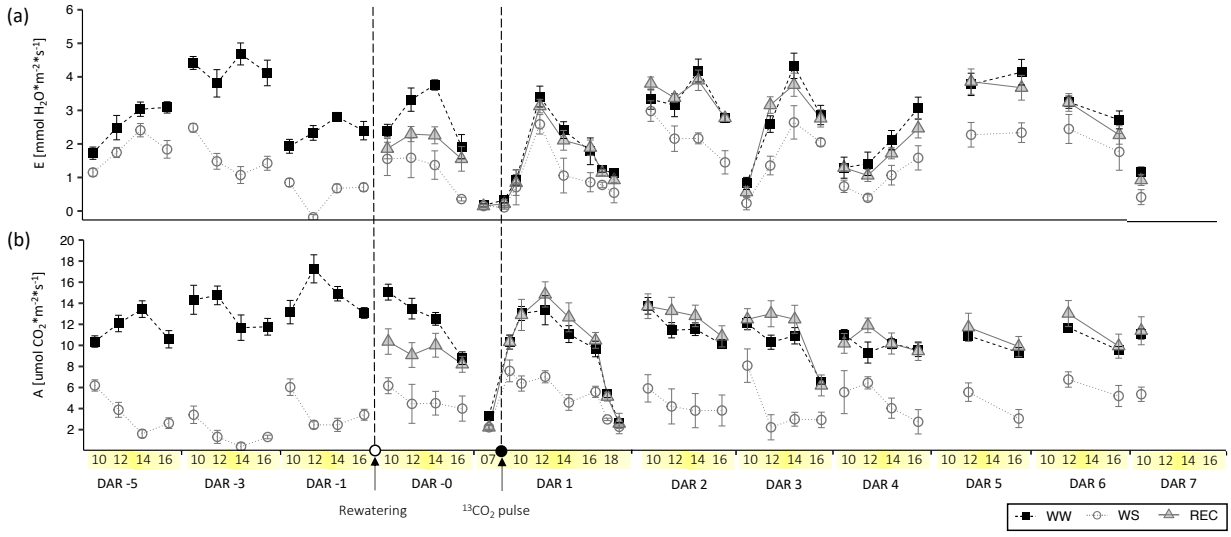


| | DAR -5 | | | | DAR -3 | | | | DAR -1 | | | | DAR 0 | | | | DAR 1 | | | | | | | | DAR 2 | | | | DAR 3 | | | | DAR 4 | | | | DAR 5 | | | | DAR 6 | | | | DAR 7 | | | |
|---|---|---|---|---|---|---|---|---|---|---|---|---|---|---|---|---|---|---|---|---|---|---|---|---|---|---|---|---|---|---|---|---|---|---|---|---|---|---|---|---|---|---|---|---|---|---|---|---|
| (a) | 10 | 12 | 14 | 16 | 10 | 12 | 14 | 16 | 10 | 12 | 14 | 16 | 10 | 12 | 14 | 16 | 7 | 9 | 10 | 12 | 14 | 16 | 17 | 18 | 10 | 12 | 14 | 16 | 10 | 12 | 14 | 16 | 10 | 12 | 14 | 16 | 10 | 12 | 14 | 16 | 10 | 12 | 14 | 16 | 10 | 12 | 14 | 16 |
| WW | a | a | a | a | a | a | a | a | a | a | a | a | a | a | a | a | a | a | a | a | a | a | a | a | ab | a | a | a | a | a | a | a | ab | a | a | a | a | | | | a | | | | a | | | |
| WS | b | b | b | b | b | b | b | b | b | b | b | b | a | b | c | b | a | a | a | b | b | b | b | b | b | b | b | b | b | b | b | b | b | b | b | b | b | | | | b | | | | b | | | |
| REC | / | / | / | / | / | / | / | / | / | / | / | / | a | b | a | a | a | a | ab | a | a | a | a | a | a | a | a | a | ab | a | a | a | a | a | a | a | a | | | | a | | | | a | | | |
| (b) | 10 | 12 | 14 | 16 | 10 | 12 | 14 | 16 | 10 | 12 | 14 | 16 | 10 | 12 | 14 | 16 | 7 | 9 | 10 | 12 | 14 | 16 | 17 | 18 | 10 | 12 | 14 | 16 | 10 | 12 | 14 | 16 | 10 | 12 | 14 | 16 | 10 | 12 | 14 | 16 | 10 | 12 | 14 | 16 | 10 | 12 | 14 | 16 |
| WW | a | a | a | a | a | a | a | a | a | a | a | a | a | a | a | a | a | a | a | a | a | a | a | a | a | a | a | a | a | b | a | a | a | b | a | a | a | | | | a | | | | a | | | |
| WS | b | b | b | b | b | b | b | b | b | b | b | b | c | c | c | b | a | b | b | b | b | b | b | a | b | b | b | b | b | c | b | b | b | c | b | b | b | | | | b | | | | b | | | |
| REC | / | / | / | / | / | / | / | / | / | / | / | / | b | b | b | a | a | a | a | a | a | a | a | a | a | a | a | a | a | a | a | a | a | a | a | a | a | | | | a | | | | a | | | |

3

1 Figure 2.
2

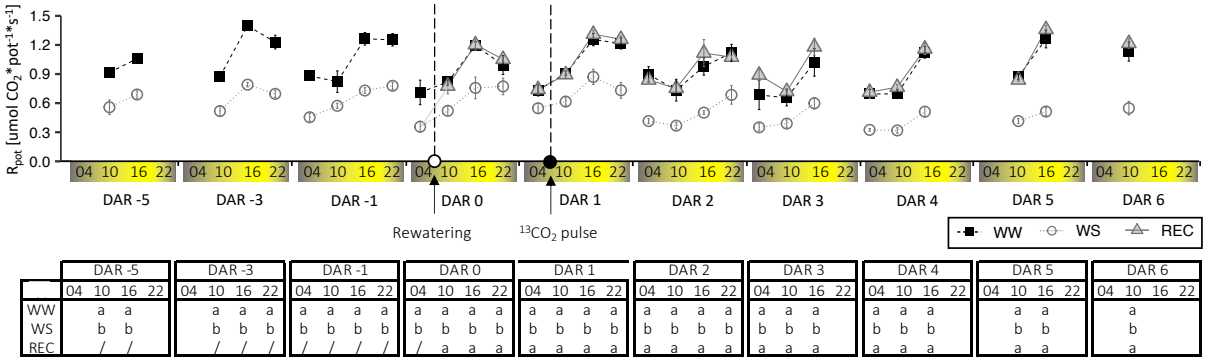


| | DAR -5 | | | | DAR -3 | | | | DAR -1 | | | | DAR 0 | | | | DAR 1 | | | | DAR 2 | | | | DAR 3 | | | | DAR 4 | | | | DAR 5 | | | | DAR 6 | | | |
|---|---|---|---|---|---|---|---|---|---|---|---|---|---|---|---|---|---|---|---|---|---|---|---|---|---|---|---|---|---|---|---|---|---|---|---|---|---|---|---|---|
| | 04 | 10 | 16 | 22 | 04 | 10 | 16 | 22 | 04 | 10 | 16 | 22 | 04 | 10 | 16 | 22 | 04 | 10 | 16 | 22 | 04 | 10 | 16 | 22 | 04 | 10 | 16 | 22 | 04 | 10 | 16 | 22 | 04 | 10 | 16 | 22 | 04 | 10 | 16 | 22 |
| WW | | a | a | | | a | a | a | a | a | a | a | a | a | a | a | a | a | a | a | a | a | a | a | a | a | a | a | a | a | a | | | a | a | | | a | | |
| WS | | b | b | | | b | b | b | b | b | b | b | b | b | b | b | b | b | b | b | b | b | b | b | b | b | b | b | b | b | b | | | b | b | | | b | | |
| REC | | / | / | | | / | / | / | / | / | / | / | / | a | a | a | a | a | a | a | a | a | a | a | a | a | a | a | a | a | a | | | a | a | | | a | | |

Figure 3.

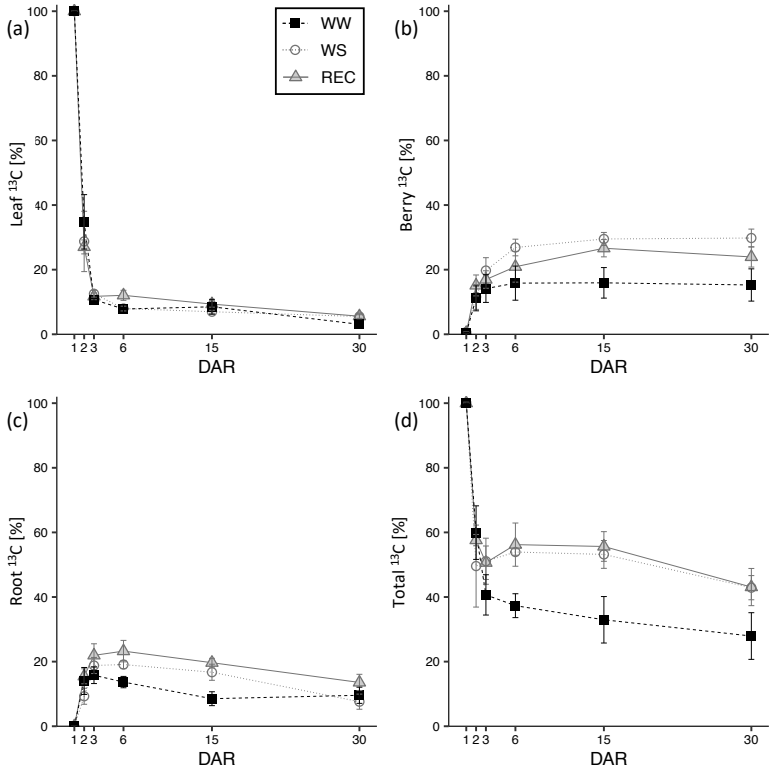


| (a) | 1 | 2 | 3 | 6 | 15 | 30 |
|---|---|---|---|---|---|---|
| WW | a | a | a | b | a | a |
| WS | a | a | a | b | a | a |
| REC | a | a | a | a | a | a |

| (b) | 1 | 2 | 3 | 6 | 15 | 30 |
|---|---|---|---|---|---|---|
| WW | a | a | a | b | b | b |
| WS | a | a | a | a | a | a |
| REC | a | a | a | ab | a | ab |

| (c) | 1 | 2 | 3 | 6 | 15 | 30 |
|---|---|---|---|---|---|---|
| WW | a | a | a | b | b | a |
| WS | a | a | a | a | a | a |
| REC | a | a | a | a | a | a |

| (d) | 1 | 2 | 3 | 6 | 15 | 30 |
|---|---|---|---|---|---|---|
| WW | a | a | a | b | b | b |
| WS | a | a | a | a | a | a |
| REC | a | a | a | a | a | a |

Figure 4.

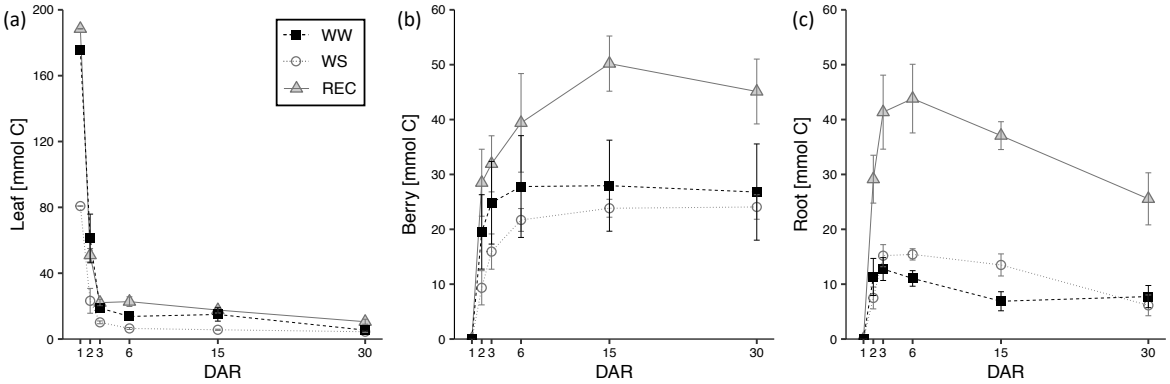


| (a) | 1 | 2 | 3 | 6 | 15 | 30 |
|---|---|---|---|---|---|---|
| WW | a | a | a | a | a | a |
| WS | b | b | b | c | b | a |
| REC | a | a | a | b | a | a |

| (b) | 1 | 2 | 3 | 6 | 15 | 30 |
|---|---|---|---|---|---|---|
| WW | a | ab | ab | ab | b | b |
| WS | a | b | b | b | b | b |
| REC | a | a | ab | a | a | a |

| (c) | 1 | 2 | 3 | 6 | 15 | 30 |
|---|---|---|---|---|---|---|
| WW | a | b | b | c | c | b |
| WS | a | b | b | b | b | b |
| REC | a | a | a | a | a | a |

Figure 5.

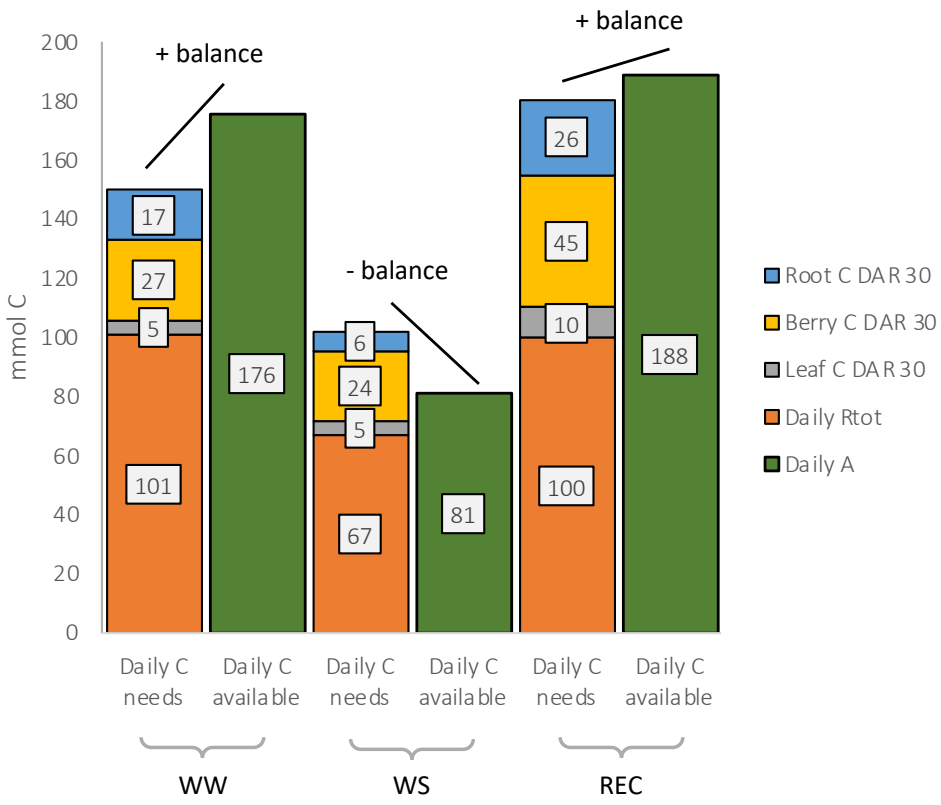
+ balance
- balance
+ balance
mmol C
200
180
160
140
120
100
80
60
40
20
0
17
27
5
101
176
6
24
5
67
81
26
45
10
100
188
Root C DAR 30
Berry C DAR 30
Leaf C DAR 30
Daily Rtot
Daily A
Daily C needs
Daily C available
Daily C needs
Daily C available
Daily C needs
Daily C available
WW
WS
REC

Figure 6.

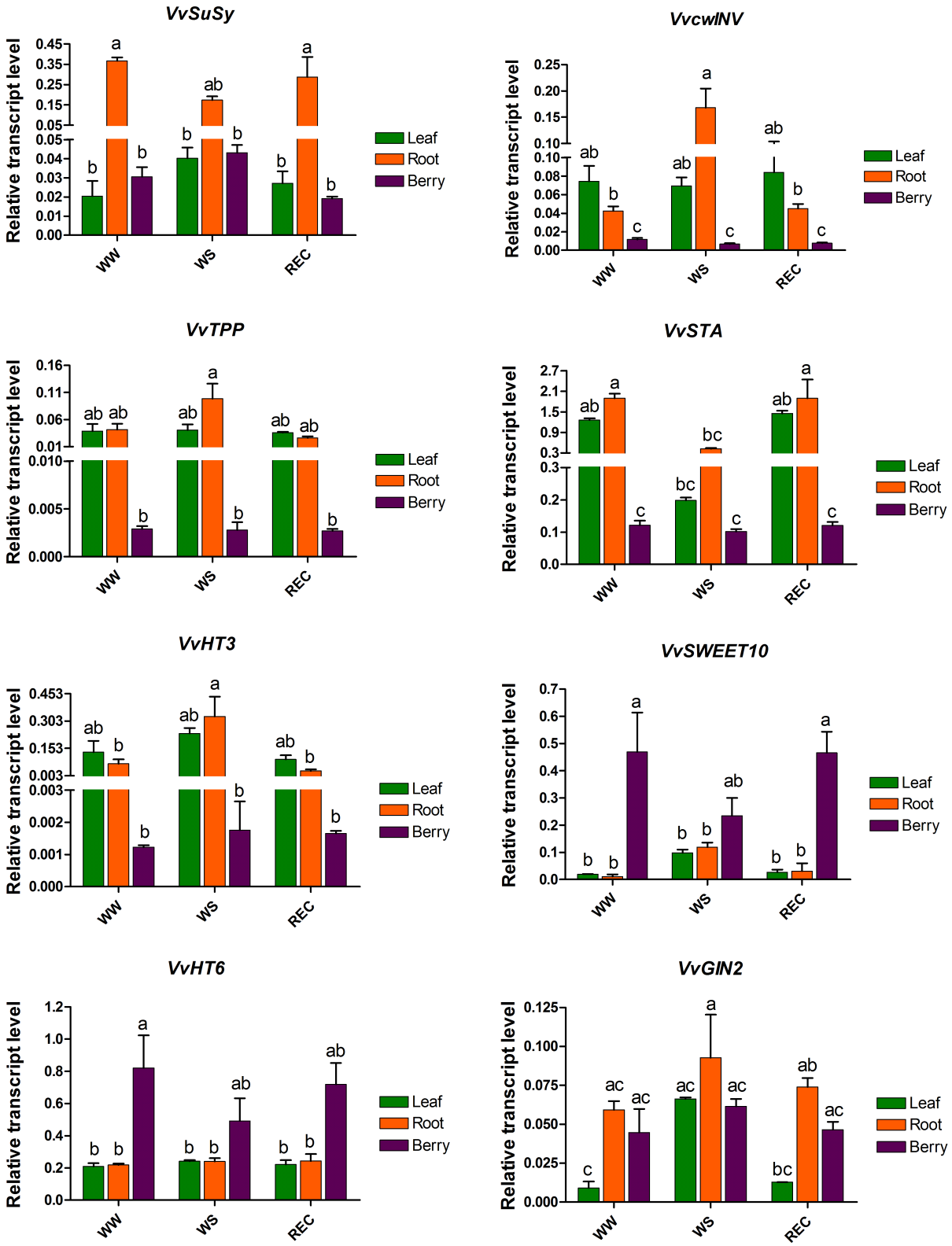
VvSuSy
VvcwINV
VvTPP
VvSTA
VvHT3
VvSWEET10
VvHT6
VvGIN2
Relative transcript level
Leaf
Root
Berry
WW
WS
REC

Figure 7.

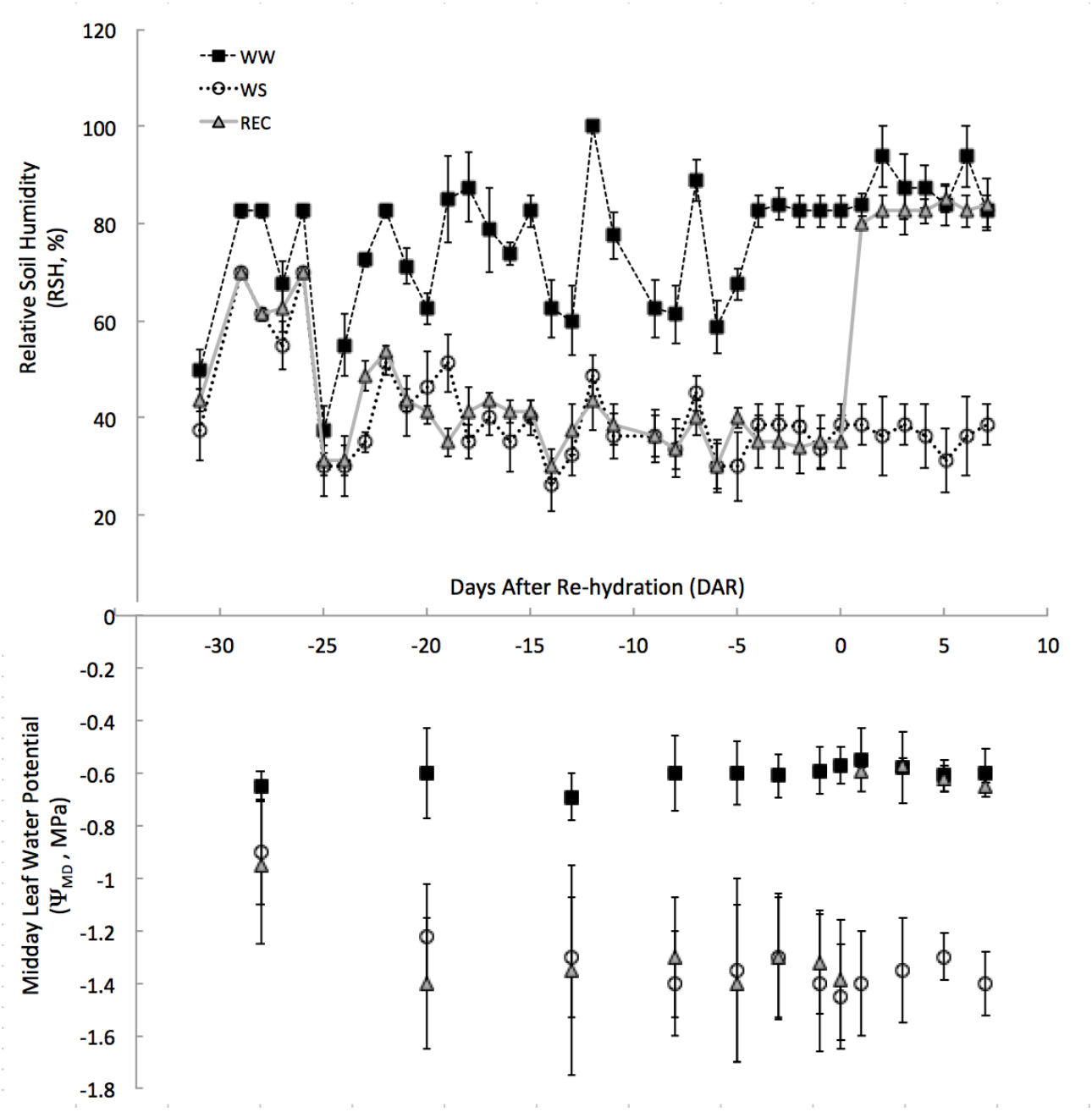
WW
WS
REC
Relative Soil Humidity (RSH, %)
120
100
80
60
40
20
0
Days After Re-hydration (DAR)
-30
-25
-20
-15
-10
-5
0
5
10
Midday Leaf Water Potential ($\Psi_{MD}$, MPa)
-0.2
-0.4
-0.6
-0.8
-1
-1.2
-1.4
-1.6
-1.8

1 Table S1.
2

| Target (Gene ID) | *Gene abbreviation* | Gene Description | Primer | Primer sequences 5'-3' | References |
|---|---|---|---|---|---|
| VIT_11s0016g00470 | *VvSuSy* | Sucrose synthase | Forward | TGTTAAGGCTCCTGGATTTCAATTA | Prezelj et al., 2016 |
| | | | Reverse | AGCCAAATCTTGGCAAGCA | |
| VIT_09s0002g02320 | *VvcwINV* | Cell wall apoplastic invertase | Forward | AGGAGGTGGAAAGGTTTGCATA | Ferrero et al., 2018 |
| | | | Reverse | TGGGCTTCACCGTCAATAGC | |
| VIT_00s0304g00080 | *VvTPP* | Trehalose-6-phosphate phosphatase | Forward | TCCATCCCAGGAGCAAGTGT | Gambino et al., 2012 |
| | | | Reverse | CACAGCGGTAATGCACAGAGA | |
| VIT_02s0025g02790 | *VvSTA* | Starch synthase | Forward | GGCGACTCTGACTGCTTCTCA | Gambino et al., 2012 |
| | | | Reverse | CCTGGGTGCCGTTGACAT | |
| VIT_11s0149g00050 | *VvHT3* | Hexose transporter 3 | Forward | AGTACGACAACCAAGGGCTACAG | Gambino et al., 2012 |
| | | | Reverse | GAGGTCAAGCCCGCAAGATA | |
| VIT_17s0000g00830 | *VvSWEET10* | Sugar Will Eventually be Exported Transporter | Forward | TATCTGCGGATTCGGTTCCA | Prezelj et al., 2016 |
| | | | Reverse | ACGCTTAGCGAGAACACGAGAC | |
| VIT_18s0122g00850 | *VvHT6* | Hexose transporter 6 | Forward | TTCTTGAAGGTGCCCGAGAC | Pagliarani et al., 2019 |
| | | | Reverse | AGTAACCTGCCTTGCTCCAAC | |
| VIT_02s0154g00090 | *VvGIN2* | Vacuolar invertase 2 | Forward | CCAACCAAGGCGATCTATG | Prezelj et al., 2016 |
| | | | Reverse | TTGAGGCAGTGATGCTGG | |
| VIT_04s0044g00580 | *VvACT* | Actin | Forward | TCCGTTCTCAGAGATCAACAA | Gambino et al., 2012 |
| | | | Reverse | ACTCTCTCATCTCAAGATATTCTATGG | |
| VIT_16s0098g01190 | *VvUBI* | Ubiquitin | Forward | TCTGAGGCTTCGTGGTGGTA | Gambino et al., 2012 |
| | | | Reverse | AGGCGTGCATAACATTTGCG | |

3
4 Supplementary Table 1. List of the oligonucleotides used in this study.
5

Figure S1.

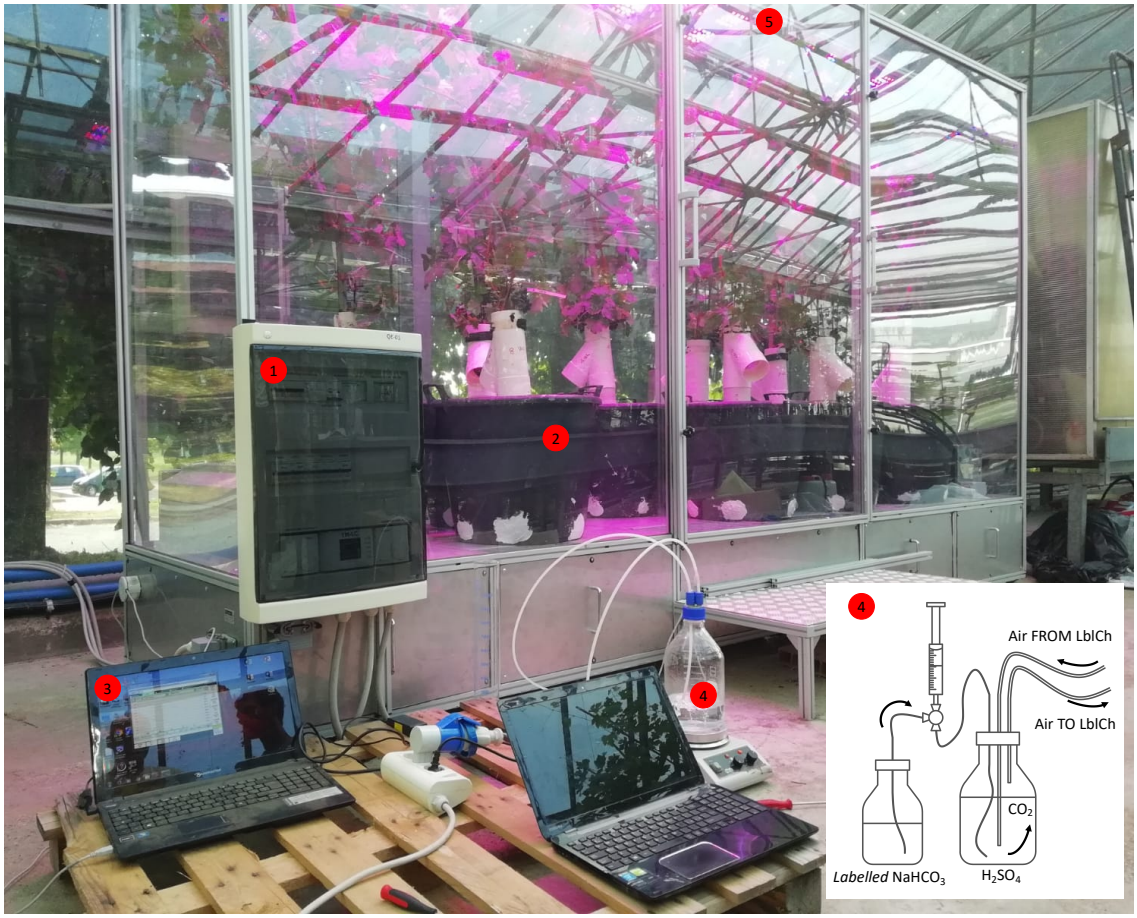


Supplementary Figure 1. $^{13}CO_2$ pulse of 9 grapevine plants under climate-controlled condition at DAR 1 in the labelling chamber. 1) Electrical panel for temperature and humidity control, 2) nine grapevines in plastic pots equipped with connection pipes and fittings for balloon setup, 3) External PC connected to the IRGA for labelling chamber $CO_2$ concentration monitoring, 4) injection system explained in the white panel 5) artificial LED light for natural light integration.

Figure S2a.

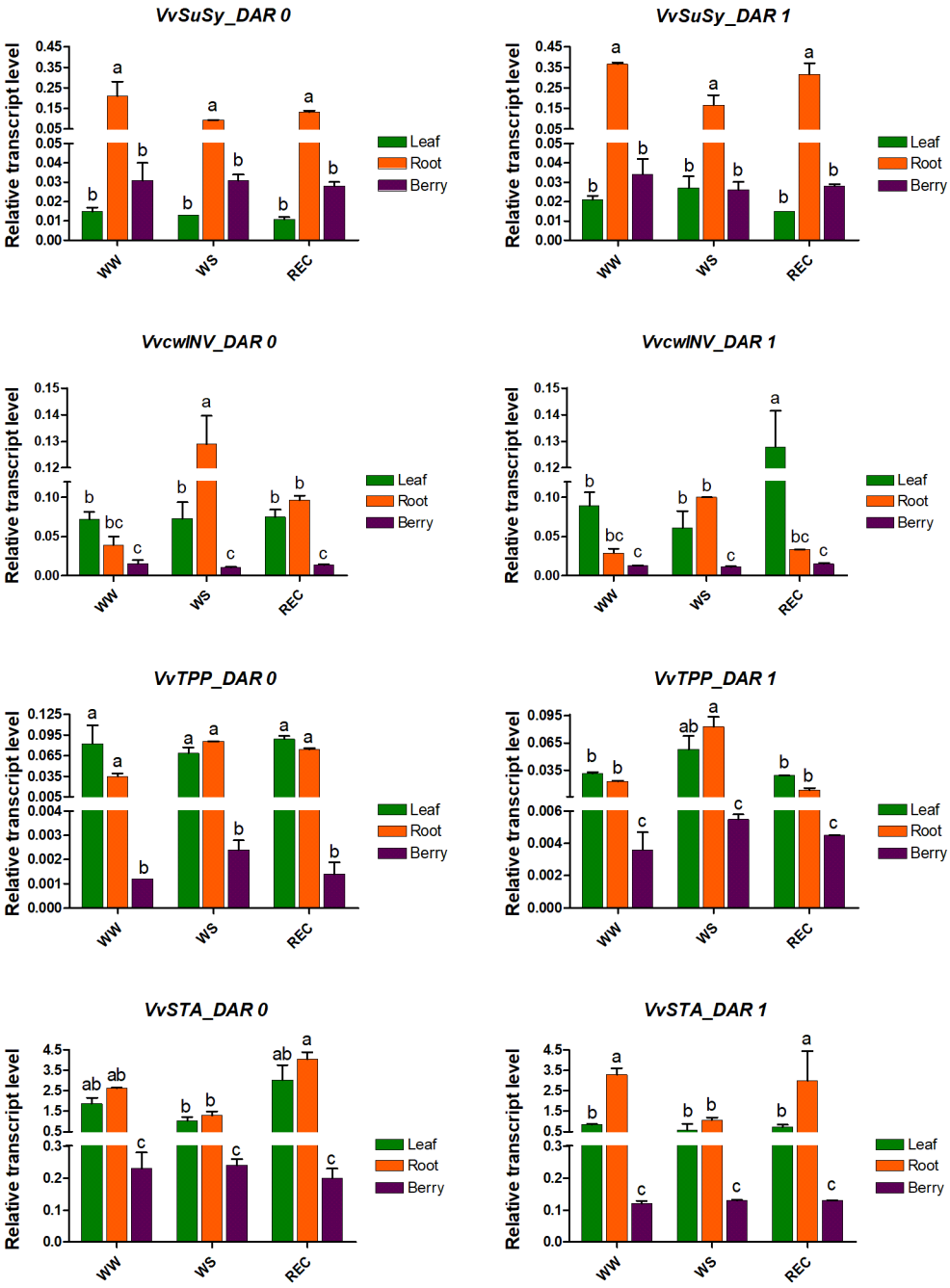
VvSuSy_DAR 0
VvSuSy_DAR 1
VvcwINV_DAR 0
VvcwINV_DAR 1
VvTPP_DAR 0
VvTPP_DAR 1
VvSTA_DAR 0
VvSTA_DAR 1
Relative transcript level
Leaf
Root
Berry
WW
WS
REC

Figure S2b.

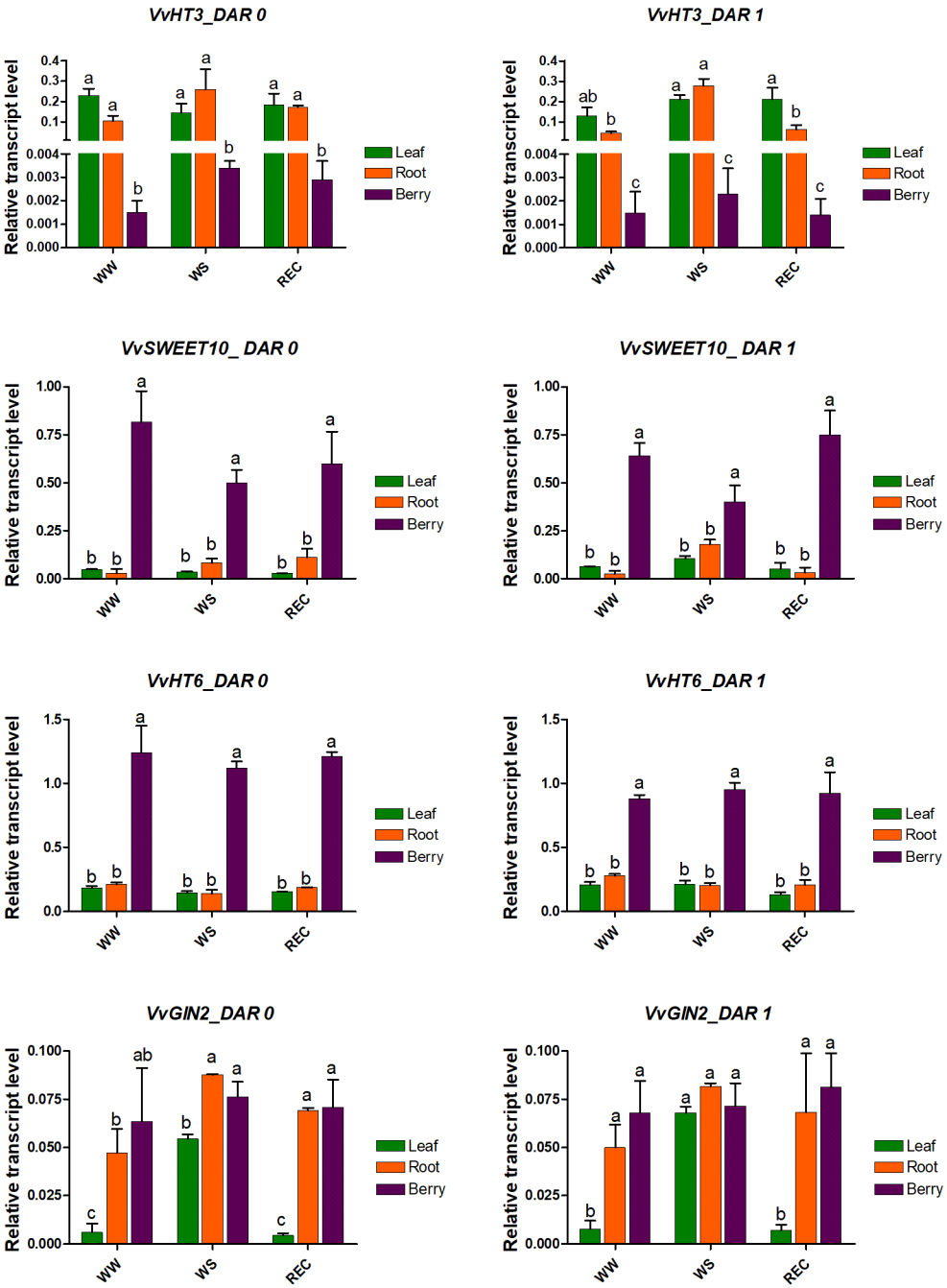


Supplementary Figure 2. Transcripts of key genes of sugar metabolism. Relative expression level of (a) sucrose synthase (*VvSusy*), cell wall invertase (*VvcwINV*), threalose-6-phosphate phosphatase (*VvTPP*), starch synthase (*VvSTA*), and (b) hexose transporter 3 (*VvHT3*), Sugar Will Eventually be Exported Transporter 10 (*VvSWEET10*), hexose transporter 6 (*VvHT6*) and vacuolar invertase 2 (*VvGIN2*) genes in leaf, root and berry tissues sampled from WW, WS and REC plants at DAR 0 and DAR1, as determined by qRT-PCR signals normalized to actin (*VvACT*) and ubiquitin (*VvUBI*) transcripts. Data are presented as the mean ±SE of three biological and technical replicates. Gene IDs and oligonucleotides used for each gene are indicated in the Table S1. Different lowercase letters above the bars indicate significant differences according to a *post hoc* Tukey's test ($p \leq 0.05$).

Figure S3.

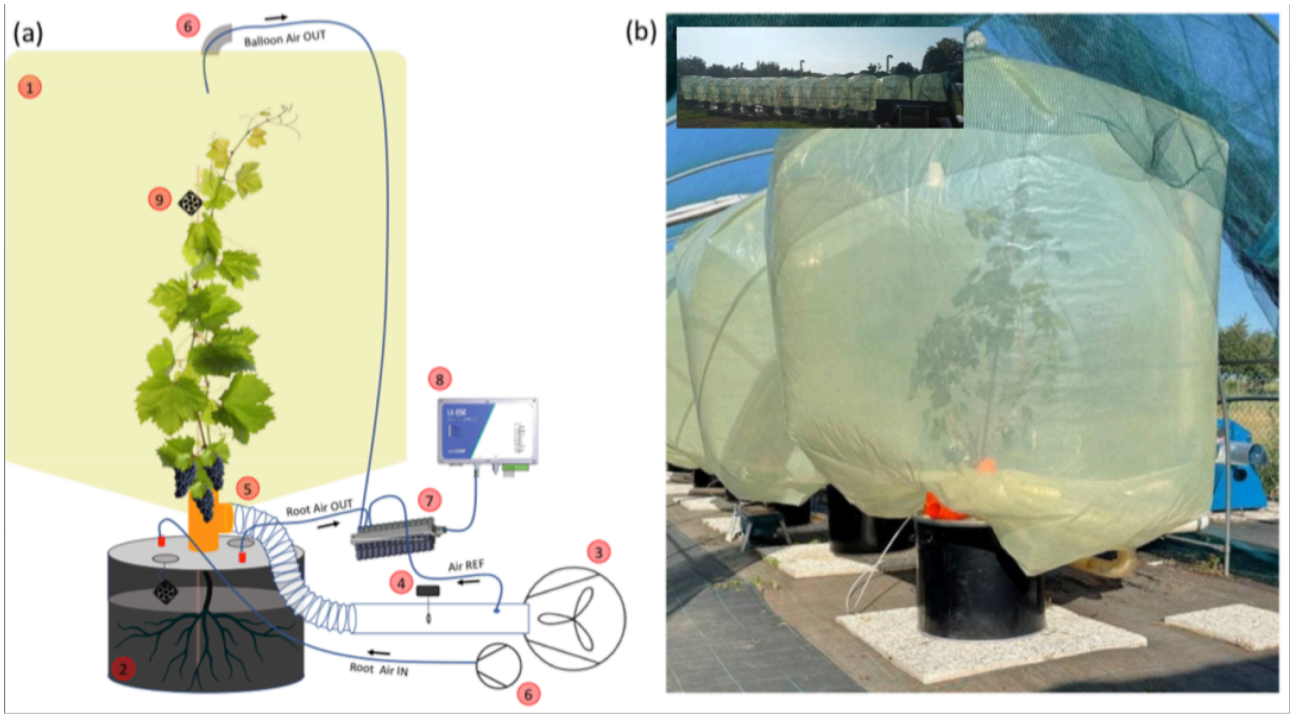


Supplementary Figure 3. Multi-chamber system for continuous gas exchange analysis. (a) schematic representation of multi-chamber system: 1) PE balloon, 2) Custom made metallic pot, 3) centrifuge fan, 4) hot-wire anemometer, 5) T junction for balloon air inlet, 6) diaphragm pump, 7) manifold with solenoid valves, 8) IRGA, 9) 12V DC fan. (b) Multi-chamber system during measurements. In the upper panel a 12-multi-chamber platform.

Figure S4.

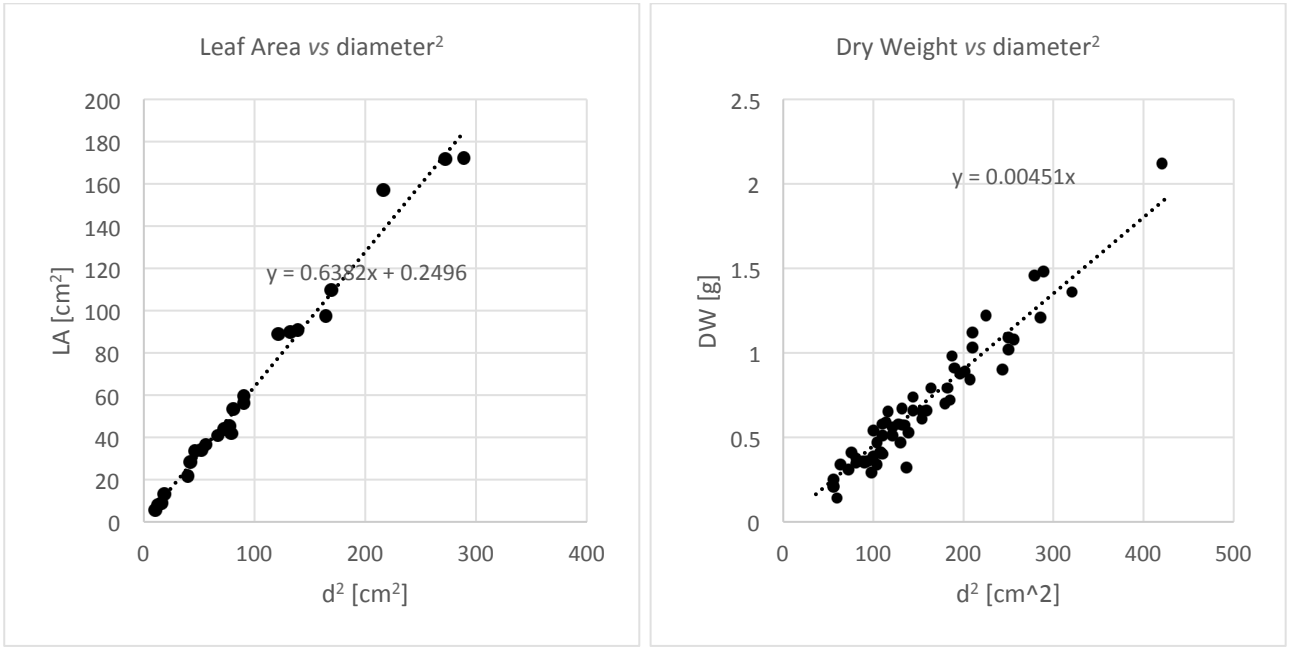


Supplementary Figure 4. Linear correlation between leaf area (LA) and leaf diameter$^2$ ($d^2$) and linear correlation between leaf dry weight (DW) and $d^2$ of *Vitis vinifera cv* Barbera grafted onto *Vitis riparia* × *Vitis berlandieri* 420A rootstocks.

Figure S5.

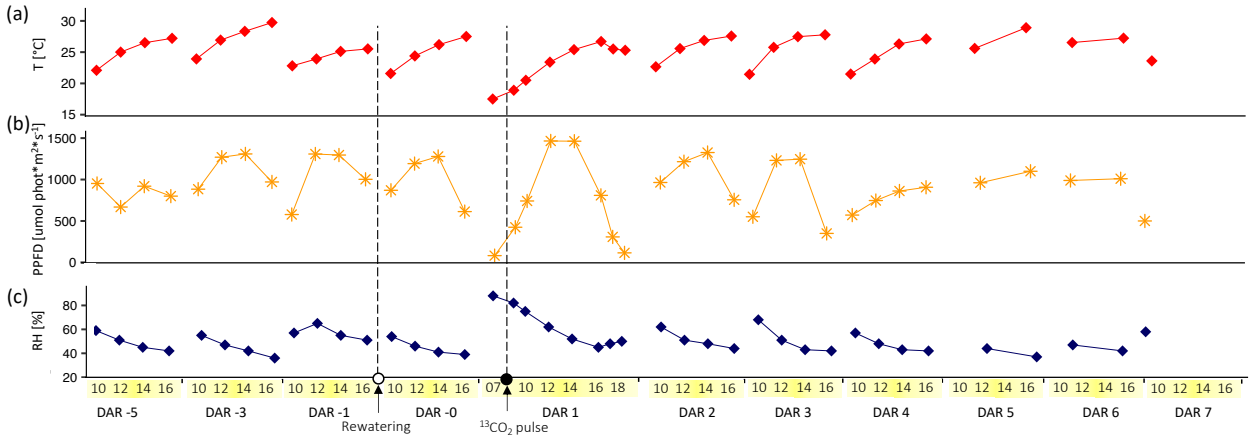


Supplementary Figure 5. Environmental check during the whole-plant gas exchange analysis. (a) air temperature, T; (b) photosynthetic photon flux density, PPFD; (c) air relative humidity, RH.